

Review

# Superhydrophobic Non-Metallic Surfaces with Multiscale Nano/Micro-Structure: Fabrication and Application

Qi Guo <sup>1,†</sup>, Jieyin Ma <sup>1,†</sup>, Tianjun Yin <sup>1</sup>, Haichuan Jin <sup>1</sup> , Jiaxiang Zheng <sup>1</sup> and Hui Gao <sup>1,2,\*</sup>

<sup>1</sup> School of Aeronautic Science and Engineering, Beihang University, Beijing 100191, China; guoqi1996@buaa.edu.cn (Q.G.); mznxmjy@buaa.edu.cn (J.M.); yintj330@163.com (T.Y.); jinhaichuan@buaa.edu.cn (H.J.); zhengjx@buaa.edu.cn (J.Z.)

<sup>2</sup> Ningbo Institute of Technology, Beihang University, Ningbo 315100, China

\* Correspondence: h.gao@buaa.edu.cn

† These authors contributed equally to this work.

**Abstract:** Multiscale nano/micro-structured surfaces with superhydrophobicity are abundantly observed in nature such as lotus leaves, rose petals and butterfly wings, where microstructures typically reinforce mechanical stability, while nanostructures predominantly govern wettability. To emulate such hierarchical structures in nature, various methods have been widely applied in the past few decades to the manufacture of multiscale structures which can be applied to functionalities ranging from anti-icing and water–oil separation to self-cleaning. In this review, we highlight recent advances in nano/micro-structured superhydrophobic surfaces, with particular focus on non-metallic materials as they are widely used in daily life due to their lightweight, abrasion resistance and ease of processing properties. This review is organized into three sections. First, fabrication methods of multiscale hierarchical structures are introduced with their strengths and weaknesses. Second, four main application areas of anti-icing, water–oil separation, anti-fog and self-cleaning are overviewed by assessing how and why multiscale structures need to be incorporated to carry out their performances. Finally, future directions and challenges for nano/micro-structured surfaces are presented.

**Keywords:** superhydrophobic surfaces; multiscale structures; non-metallic materials; fabrication methods; applications



**Citation:** Guo, Q.; Ma, J.; Yin, T.; Jin, H.; Zheng, J.; Gao, H.

Superhydrophobic Non-Metallic Surfaces with Multiscale Nano/Micro-Structure: Fabrication and Application. *Molecules* **2024**, *29*, 2098. <https://doi.org/10.3390/molecules29092098>

Academic Editor: Apostolos Avgeropoulos

Received: 8 February 2024

Revised: 19 April 2024

Accepted: 25 April 2024

Published: 1 May 2024



**Copyright:** © 2024 by the authors. Licensee MDPI, Basel, Switzerland. This article is an open access article distributed under the terms and conditions of the Creative Commons Attribution (CC BY) license (<https://creativecommons.org/licenses/by/4.0/>).

## 1. Introduction

A superhydrophobic non-metallic surface refers to surfaces engineered to exhibit an extremely high water contact angle (WCA,  $\theta$ ) with no less than  $150^\circ$  through surface modification techniques [1]; these surfaces play an indispensable role in our daily life and can be found in applications across diverse sectors of daily necessities, architecture, healthcare, textiles, transportation and environmental conservation [2–15].

The concept of surface modification to enable superhydrophobicity is derived from the lotus effect [16]. The upper surface of the lotus leaf possesses an excellent water-repellency property as a result of its well-organized hierarchical structures from the nano to the micrometer scale and a wax-like coating that contributes to a large contact angle and a small roll-off angle. This observation reveals two crucial characteristics for achieving superhydrophobicity on a solid surface, nano/micro-structured topography and a low surface energy [17,18]. Among them, nano/micro-structured topography pertains to the array of concave–convex structures occurring at micro- and nano-scales, resulting in a reduction in the contact area between the liquid and the surface. Meanwhile low surface energy refers to a weak interactive force between surface molecules, making the surface resistant to wetting or covering by other substances. A similar phenomenon, additionally, is also observed on the surfaces of pitcher plants [19], water strider legs [20], rose petals [21], rice leaves [22] and other creatures. Such findings further promote the development and investigation of biomimetic superhydrophobic surfaces because of their outstanding

performances and potential applications including, but not limited to, anti-icing [23,24], anti-fogging [25,26] and self-cleaning [27,28].

Such surfaces with multiscale hierarchical structure which possess excellent superhydrophobicity can be theoretically well explained. As early as 1805, Young's equation [29] described the relationship between WCA and surface energy at the solid–liquid–gas three-phase interface, as shown in Equation (1):

$$\gamma_{LV}\cos\theta_Y = \gamma_{SV} - \gamma_{SL} \quad (1)$$

where  $\gamma_{SV}$ ,  $\gamma_{LV}$  and  $\gamma_{SL}$  represent the free energy per unit area at the solid–liquid interface, liquid–gas interface and solid–gas interface, respectively.  $\theta_Y$  denotes the Young's angle. This equation indicates that a lower solid–liquid surface energy results in a higher contact angle. However, the actual surfaces are not absolutely smooth. To better account for surface roughness, the Wenzel model [30] and Cassie–Baxter model [31] were introduced and widely recognized for elucidating the phenomenon of superhydrophobicity on complex structures [32], as illustrated in Figure 1A. In practice, the actual wettability of surfaces lies between the extremes described by the Wenzel and Cassie–Baxter models, referred to as the mixed Cassie–Wenzel model (Figure 1A), where the liquid partially wets the rough surface structure [33]. In such cases, the contact angle can be analyzed by Equation (2).

$$\cos\theta_{C-W} = f_1(r\cos\theta_Y + 1) - 1 \quad (2)$$

where  $\theta_{C-W}$  represents the apparent contact angle,  $f_1$  is the proportion of the contact area between the liquid droplet and the rough surface, and  $r$  denotes the surface roughness. Building upon the foundation of low surface energy, this model further introduces a key parameter of superhydrophobicity, the small solid–liquid contact area, which can be achieved by constructing multiscale nano/micro-structures on the surface. Multiscale structures, as depicted in Figure 1B, can create more micro cavities and protrusions in contrast to simple rough micro-structures, leading to a smaller solid–liquid contact area. This aids in capturing more air on the surface, forming micro air pockets. Meanwhile, nano structures with high aspect ratios are mechanically fragile [34], whereas micro-scale protrusions have higher mechanical stability [35]. A combination of the two can create a surface with excellent superhydrophobicity and high robustness, offering more possibilities for surface structure design [36,37].

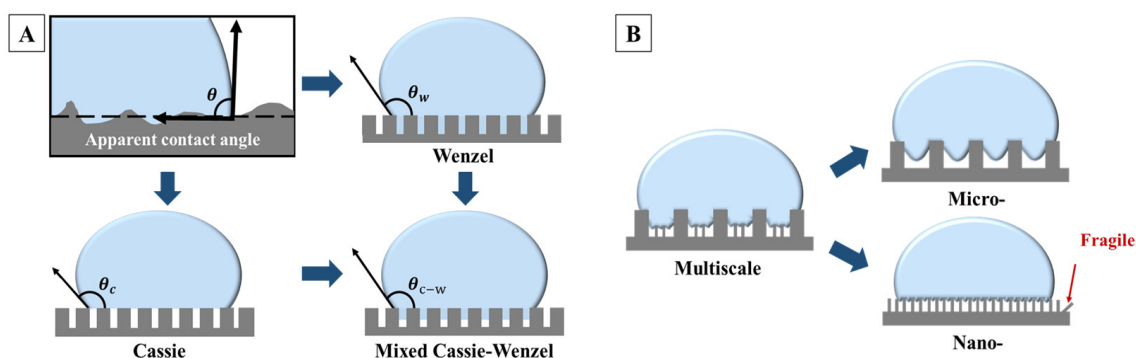


**Figure 1.** (A) The apparent contact angle  $\theta$ , and a schematic diagram of Wenzel's model, Cassie–Baxter's model, and the mixed Cassie–Wenzel model. (B) A schematic diagram of the difference between multiscale structures and single micro-structures and single nano-structures.

Superhydrophobic modification via multiscale structures is therefore the focus of current research, with a continuous influx of novel findings. The multiscale nano/micro-structure enhances the material surface with a higher contact angle and stronger water-repellency. However, compared with a single structure, the preparation process of nano/micro-structures is more complex, requiring precise processing technology and material

design. Researchers have developed various methods such as the sol–gel technique, the etching method, etc., to fabricate concave–convex structures occurring at micro- and nano-scales for different applications. Substrates with diverse material compositions can be designed and modified with multilevel nano/micro-structures to achieve superhydrophobicity. Non-metallic materials offer advantages such as eco-friendliness and lower costs compared to metallic materials. The demand for superhydrophobic non-metallic surfaces is increasing in various fields, including construction, automotive, aerospace and medical industries. For instance, superhydrophobic modification of transparent materials like inorganic glass or organic polymers can prevent fogging, improve self-cleaning ability and enhance safety of use [38]. In applications involving composite materials, such as wind turbine blades and aircraft wings, using superhydrophobicity to prevent icing has become a recent research focus [39,40]. In the field of oil–water separation, non-metallic materials are gradually replacing metallic ones due to their excellent corrosion resistance and environmental friendliness, becoming the topics of current interest [41,42]. It is evident that there is a high demand for superhydrophobic non-metallic surfaces across different industries. Despite this demand, there exists a dearth of systematic summarization of methods for superhydrophobic surface modification with multiscale nano/micro-structures in non-metallic materials.

Hence, this review systematically summarizes the latest research, the common methods and the application prospects of the superhydrophobic non-metallic surfaces with nano/micro(multiscale)-structures, as shown in Figure 2, which will make an important contribution to the production and utilization of superhydrophobic surfaces on non-metallic materials, and the preparation of multiscale structures on the surface of non-metallic materials.

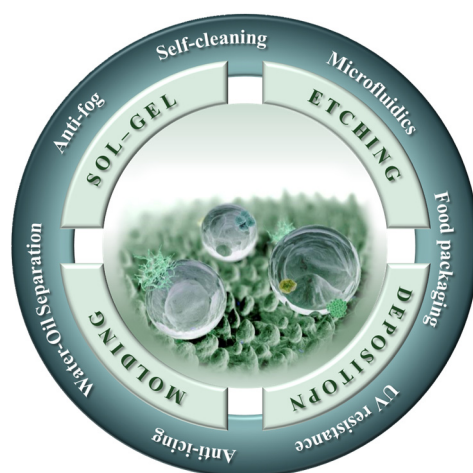


**Figure 2.** A schematic diagram illustrating the different preparation methods and applications of the superhydrophobic non-metallic surfaces with nano/micro(multiscale)-structures discussed in this review [43].

## 2. Preparation Methods of Nano/Micro-Structured Superhydrophobic Surfaces

To achieve superhydrophobic surfaces with unique wettability and structures, a variety of techniques have been employed. Previous research has mainly concentrated on enhancing superhydrophobicity. However, with the development of technology, besides superhydrophobicity, people have started to pay more attention to the overall performance of superhydrophobic surfaces, such as robustness and large-scale preparation. Consequently, higher demands are being placed on the preparation technology. In this section, the preparation techniques of non-metallic surfaces with multiscale nano/micro-structures are mainly concerned. Various common techniques are introduced respectively, which can be mainly divided into physical and chemical methods [44,45]. Physical methods include etching, molding and physical vapor deposition (PVD) to form microscopic and nano-scale structures on the material surfaces through precision machining or by using

a stencil [46,47]. Chemical methods include the sol–gel method, chemical vapor deposition (CVD) and electrochemical deposition (ECD), which change the surface energy and structure by depositing or synthesizing compounds on the surfaces [48–50]. These methods can be applied individually or in combination to meet the needs of multiscale nano/micro-structured superhydrophobic surfaces for different applications.

### 2.1. Sol–Gel Method

The sol–gel method stands as a prevalent technique for the preparation of wet chemical materials [51]. In this process, the precursor undergoes hydrolysis in the liquid phase, leading to the formation of a gel system through the condensation polymerization of colloidal particles [52,53]. Then, the nano-particles in the gel system can be adsorbed on the substrate, forming a thin film combined with the surface of the substrate material [54–56]. Another way is to manage the gel system by using heat treatment to obtain treated nano-particles [57] and then cover the surface by using physical methods such as the spraying method or the dip-coating method. The schematic diagrams of the two routes are shown in Figure 3. In addition, the superhydrophobic properties can also be further enhanced or functionalized through chemical modification. The sol–gel method offers a well-established route for creating superhydrophobic surfaces on non-metallic substrates [58]. Despite limitations in morphology controllability through spraying or dipping [59,60], it still provides a versatile platform for doping new materials and is compatible with various substrates [61–63], enhancing the possibilities of the surface design. Nonetheless, due to its numerous advantages, the sol–gel method remains one of the important methods for preparing superhydrophobic surfaces with multiscale structures on non-metallic materials.

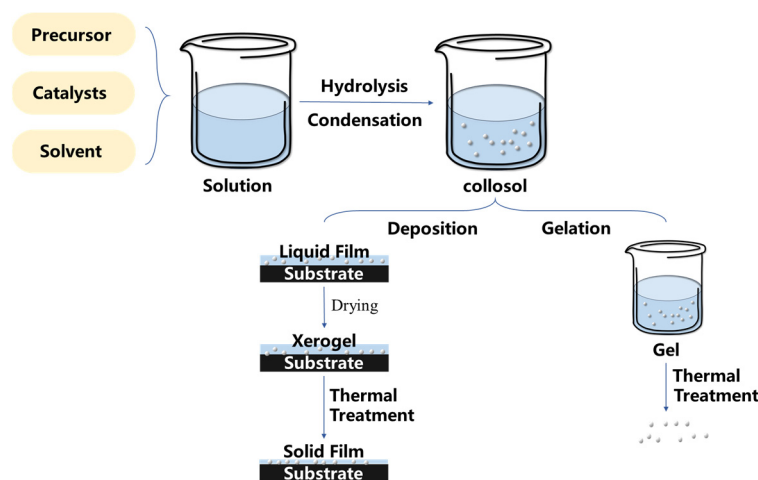


**Figure 3.** A diagram of the main steps in a typical sol–gel process.

Superhydrophobic surfaces with different non-metallic compositions can be facily produced by the sol–gel method. For example, silica and titania coatings are common materials used for superhydrophobic surface modification through the sol–gel method [64–68]. By means of the classical Stöber process [52,69–73], as depicted in Figure 4A, Heiman-Burstein et al. [74] achieved a superhydrophobic coating by modifying silica nano-particles through the in situ addition of long-chain alkyl silane co-precursors, in combination with tetraethyl orthosilicate (TEOS). They discovered that when the alkyl length exceeded ten carbons, a superhydrophobic coating could be achieved, showcasing a raspberry-like hierarchical morphology. The direct condensation of silica nano-particles (NPs) on the substrate surface results in covalent bonding between the TEOS/alkyl silane systems and compatibilized (oxygen-treated) substrates. This covalent bonding facilitates the attachment of the silane-treated particles to the substrate, enhancing the coating’s durability. Wang et al. [75] also prepared silica modified cellulose fibers via a modified Stöber method, obtaining a hierar-

chical superhydrophobic surface with a WCA up to  $151.3^\circ$ . As for the titania coating, Hu et al. [76], inspired by the reversible swelling ability of cured rubber, immersed the swollen silicone rubber (SR) in a tetrabutyltitanate (TBT) solution (precursor of sol-gel). The precursor moved into the SR and came into contact with the catalyst, resulting in the generation of  $\text{TiO}_2$  particles in the crosslinking network of SR. The  $\text{TiO}_2$  particles grew gradually and formed a texture of multiscale roughness on the SR surface, which is shown in Figure 4B, with a WCA and a roll-off angle of  $158.6^\circ$  and  $6.5^\circ$ . The embedding of  $\text{TiO}_2$  particles in SR enhanced the mechanical durability of the superhydrophobic surfaces compared to samples prepared by conventional sol-gel methods. Nasiri Khalil Abad et al. [77] also designed a Cd-Si co-doped  $\text{TiO}_2$  thin film, in which titania nanoparticles were synthesized by the sol-gel method. The results illustrate that the increasing calcination temperature triggered the agglomeration of particles, which induced a WCA of nearly  $168^\circ$  on the surface.

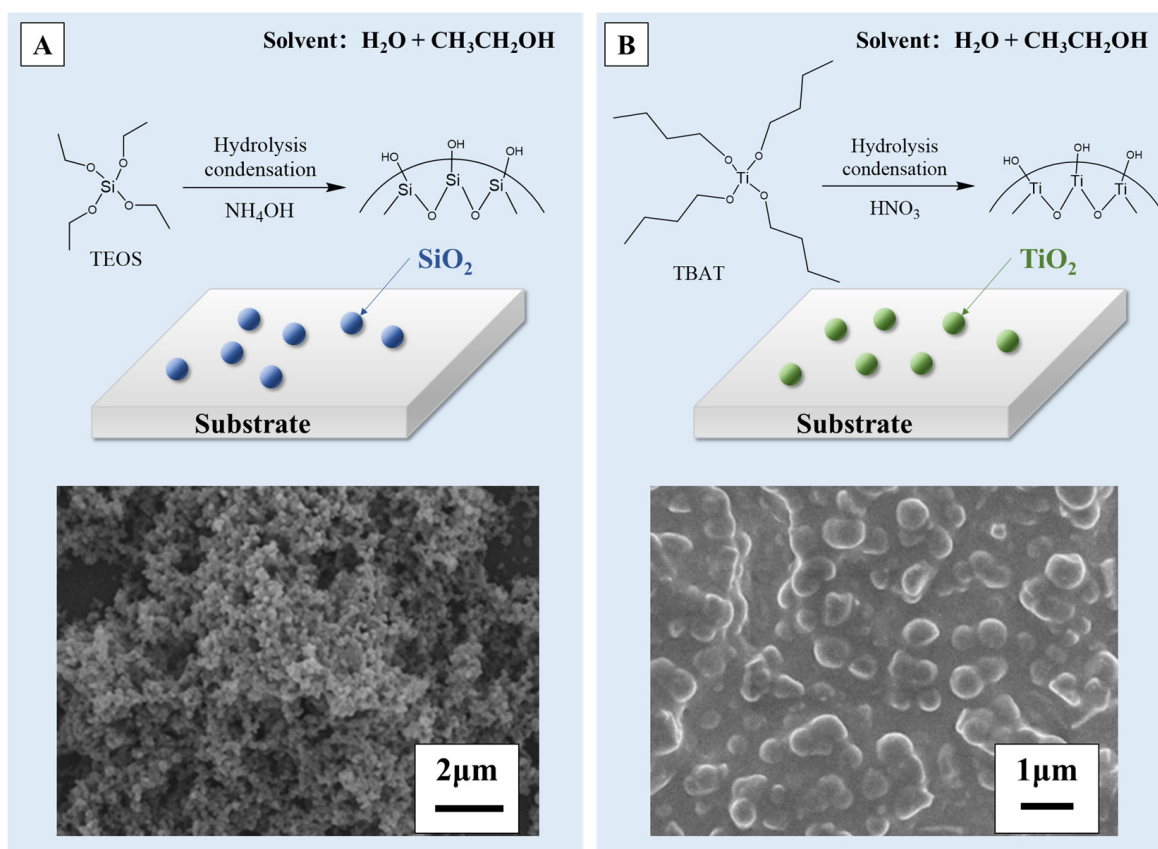


**Figure 4.** A schematic illustration and scanning electron microscope (SEM) image of (A)  $\text{SiO}_2$  [74,75] and (B)  $\text{TiO}_2$  coatings [76] prepared by the sol-gel method. Reprinted with permission from [74–76], Copyright 2021 MDPI, Copyright 2019 MDPI, Copyright 2020 Elsevier, respectively.

The gel can also serve as a functional adhesive material, adhering other nano-particle fillers to the surface [78,79]. The combination of the two forms of nano/micro-structures induced superhydrophobicity on the surface. Zhou et al. [80] prepared the siloxane zwitterionic compound (GPAC) through a modified sol-gel method, mixing it with carnauba wax micro-particles to obtain a clear colloidal suspension (W-GPAC). The wax displayed a spherical structure with large pores throughout the surface. Meanwhile, the GPAC sol showed a wrinkled structure, and the “close-packed” layered structure could be observed in the W-GPAC composite, which could be beneficial due to its durability and good mechanical property. Experimental tests indicate that the surface’s WCA can reach  $170^\circ$ , demonstrating outstanding superhydrophobicity. Meanwhile, the amine group within the W-GPAC sol can form hydrogen bonds with the substrate, while 3-Glycidyloxypropyltrimethoxysilane (KH-560) facilitates excellent adhesion through a coupling reaction during the coating’s curing

process. These mechanisms collectively enhance the adhesion between the coating and the substrate. Likewise, Patra et al. [81] used silica as a nano-particle filler, mixed it in the gel system with 1*H*,1*H*,2*H*,2*H*-perfluoro-octyltriethoxysilane (FTS), and deposited it onto the substrate to form nano/micro-structures.

In recent years, significant advancements in achieving high superhydrophobicity have been demonstrated by superhydrophobic coatings prepared via the sol–gel method. Researchers in the field are now gradually exploring methods to enhance the robustness and durability of these coatings, such as physical methods (e.g., embedding) and chemical methods (e.g., bonding). This provides a new idea for subsequent research on multiscale superhydrophobic surfaces and further improves the reliability of superhydrophobic coatings.

## 2.2. Etching Methods

Etching methods are a common technique utilized for the preparation of multiscale-structured superhydrophobic surfaces [82] which can precisely control the surface structure and morphology by etching the substrate, such as through chemical etching, laser etching, electrochemical etching and plasma etching [83–85]. To achieve superhydrophobicity, the etched substrates are then modified by low-surface-energy materials [46]. It should be mentioned that chemical etching and electrochemical etching are mainly applied to metallic materials, so they are not discussed in this work. In contrast, physical etching methods such as laser etching and plasma etching are generally used for non-metallic materials, so they are discussed in detail as follows.

### 2.2.1. Laser Etching Method

The laser etching method [86] works by directing a high-energy laser beam onto the material surface, causing a series of reactions such as melting and vaporization under the action of photoelectric or photothermal effects and finally forming rough multiscale nano/micro-structures. Due to the excellent controllability of laser etching, this method can be used to etch nano/micro-structures on thin surfaces [87], such as the oxidized graphene film [88] and the polydimethylsiloxane (PDMS) film [89]. For example, when the oxidized graphene film was overlaid on a fabric surface and subjected to double-laser interference ablation, graphene nano-structures were generated by deoxygenation at the ablated locations (Figure 5A). This, in conjunction with the larger micrometer-scale structures of the underlying fabric, forms a nano/micro-multiscale graphene surface, resulting excellent superhydrophobicity [88].

The size and shape of multiscale nano/micro-structures can be controlled by changing the laser parameters or by controlling the position, energy and frequency of the laser etching. Thus, columnar, channel, stepped and other different pattern structures are prepared on the substrate surfaces [89–91]. Fang et al. [92] used femtosecond laser ablation technology to construct a micro-groove array structure on the surface of PDMS and further introduced nano/micro-step structures (Figure 5B) by adjusting the laser etching times at different positions. Wang et al. [93], inspired by the nano/micro-structures on the surface of *Oxalis corniculata* Linn., used an ultraviolet (UV) laser (355 nm) and CO<sub>2</sub> laser (10.64 μm) to etch polyimide (PI) films sequentially, and a jigsaw-like micro-structure was obtained (Figure 5C). The structure and porous graphene constituted the three-dimensional multiscale structure of the surface, and a multiscale biomimetic graphene surface was obtained.

### 2.2.2. Plasma Etching Method

Plasma etching utilizes high-frequency glow discharge reactions, activating reaction gases into reactive particles that diffuse to the etching site. Upon inter-reacting with the etched material, volatile by-products are generated and eliminated subsequently, achieving the purpose of etching [45,94,95]. Compared to laser ablation methods, plasma etching has higher dimensions but lower precision, often requiring the assistance of surface molds or oxide layers [35]. Ko et al. [96] proposed a one-step approach using metallic mesh masking. Through a plasma selective etching process assisted by double-scale etching mold, they

prepared a layer-structured superhydrophobic surface (Figure 5D). By controlling the gap distance between the substrate and the metallic mesh, the dual-scale etching masking effect was achieved, achieving a water contact angle of up to  $164.1^\circ$ . Zhang et al. [97] developed superhydrophobic cotton fabric through a process involving oxygen plasma etching followed by the application of a hydrophobic suspension containing  $\text{SiO}_2$  nanoparticles via spraying. The  $\text{SiO}_2$  nanoparticles were deposited on the fiber, which together with the uniform strip grooves created by plasma etching contributed to a dual-scale rough structure on the fabric surface.

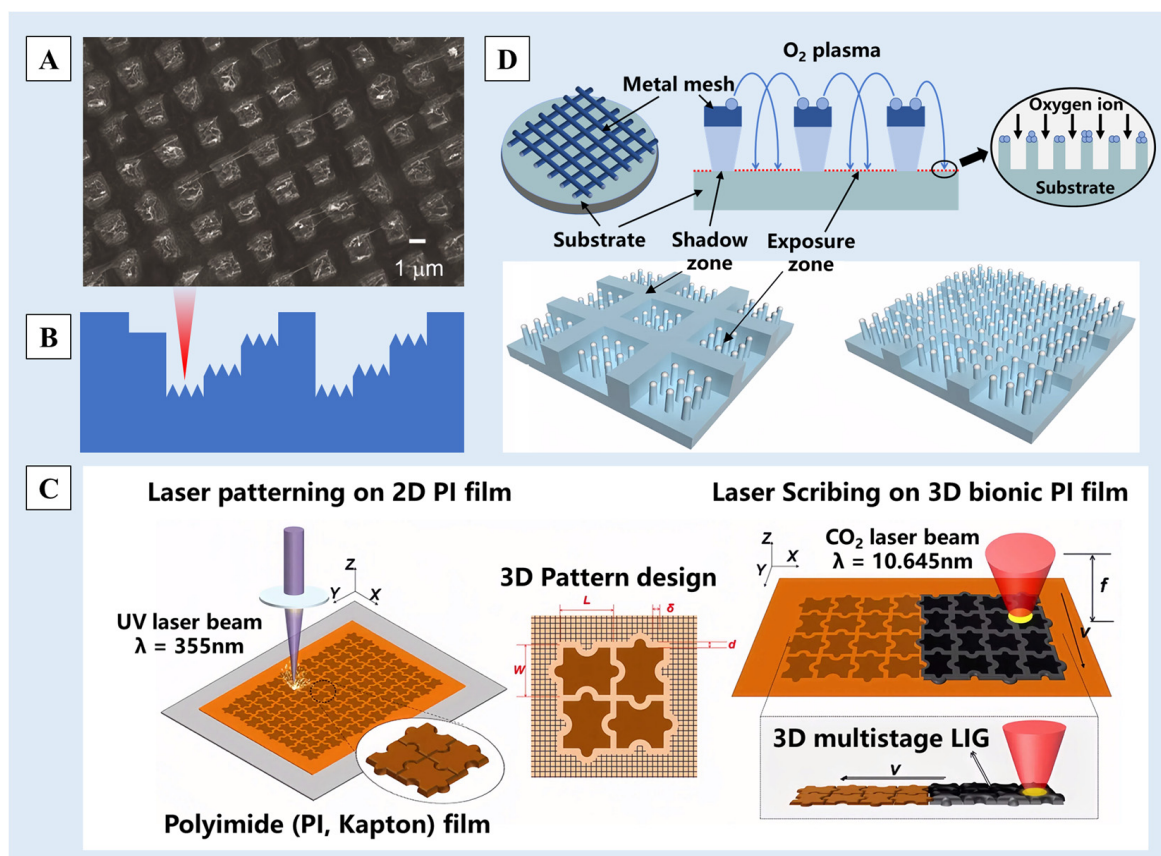


**Figure 5.** (A) A SEM image of the graphene structure produced with 0.8 W laser power [88]. (B) The stepped structure produced by adjusting the laser etching times [92]. (C) A schematic illustration of a jigsaw-like laser-induced graphene (LIG) fabricated by laser patterning on a pure PI film and then by laser scribing on a three-dimensional (3D) bionic PI film [93]. (D) Illustrations of a hybrid patterning process assisted by a metal mesh overhang showing two characteristic etching masks [96]. Reprinted with permission from [88,92,93,96], Copyright 2019 SciEngine, Copyright 2018 John Wiley and Sons, Copyright 2022 Springer Nature, Copyright 2020 Springer Nature, respectively.

Etching methods have high processing precision and good controllability, which can accurately control the surface microscopic shape and prepare complex multiscale nano/micro-structures [85,98], thus improving the superhydrophobicity, and they are suitable for a variety of non-metallic materials. However, the equipment is expensive and the processing cost is high [50], which is not suitable for industrial large-scale production. Among them, plasma etching is more efficient than laser etching, while laser etching is more environmentally friendly [46].

### 2.3. Molding Method

The molding method [99–101] involves depositing the target material on the natural or artificial template to reproduce the rough structure of the template. As early as 2009,

researchers attempted to use the molding method to prepare superhydrophobic surfaces and successfully obtained polymer surfaces with a contact angle of  $167^\circ$  [102]. In recent years, the micro-structure of superhydrophobic surfaces prepared by the molding method has gradually developed from single-scale roughness to a double-scale micro-structure to enhance the mechanical durability of the surface. And the multiscale superhydrophobic surface can be produced on a large scale. The key with the molding method is the preparation of defect-free molds, which can be typically achieved through methods such as etching or 3D printing.

Photolithography [103] and chemical etching [104] are common methods for making molds. The specific scale molds are produced by photoetching or chemical etching, and then, the required raw materials are affixed to the mold surface, resulting in the creation of a superhydrophobic surface with a nano/micro-structure. As shown in Figure 6A, Choi et al. [105] proposed a directional photofluidization imprint lithography (DPIL) method, in which polydisperse orange 3 (PDO 3) and bisphenol A-type epoxy resin were used as raw materials to make thin-film materials and then silicon molds of different scales were prepared by photolithography. The raw materials were polymerized and cured in different molds many times, following by being bonded to the surface of the film to form the multiscale nano/micro-structure. As shown in Figure 6B, a two-step template approach was used to create flexible molds with hierarchical nano/micro-structures on the surface, with anodic porous alumina serving as a starting material. On the surfaces of tubular substrates and convex lenses, ordered pillar arrays with hierarchical nano/micro-structures may be created by photo-nanoimprinting utilizing the acquired flexible molds [106]. In recent years, with the development of 3D printing technology, researchers have tried to use this method to make molds [107]. Li et al. [108] prepared a silicone hot film with elasticity and shape memory at a high temperature in the 3D printing mold, and made T-shaped grooving on it. The perfluoropolymer material coated on any surface was pressed with the mold at  $280^\circ\text{C}$ , resulting in a multiscale superhydrophobic structure of the monolithic perfluoropolymer surface (MPS) with a contact angle up to  $160^\circ$  (Figure 6C).

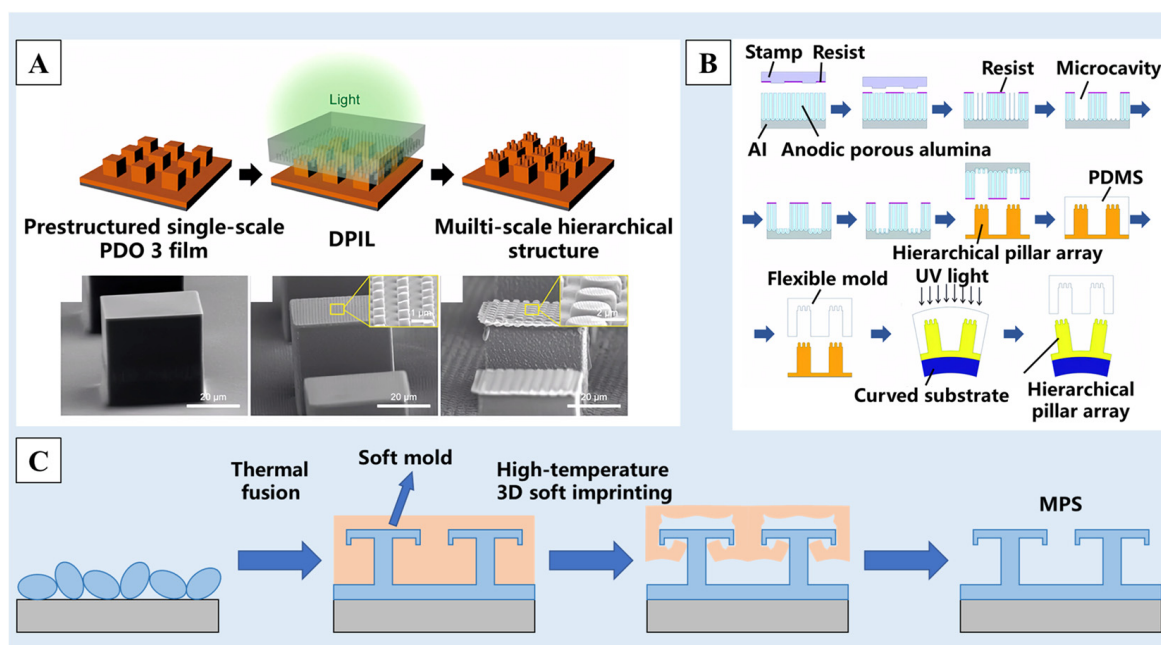


**Figure 6.** (A) Multiscale hierarchical structures formed by DPIL [105]. (B) The states of a droplet on surfaces of different roughness: micro-papillae, sub-mm papillae and hybrid papillae [106]. (C) A schematic illustration of the fabrication method consisting of thermal fusion and high-temperature 3D soft imprinting [108]. Reprinted with permission from [105,106,108], Copyright 2017 American Chemical Society, Copyright 2022 RSC Publishing, Copyright 2023 Elsevier, respectively.

In addition to the above methods for preparing templates, some researchers have directly used existing materials with rough surface structures as templates, such as stainless steel mesh [109], woven fiber cloth [110], etc. As shown in Figure 7A, He et al. [109] used stainless steel mesh as a template and silicone rubber as a raw material, and transferred the structure of the stainless steel mesh to the surface of the silicone rubber through the template method to build a surface structure. Then, the surface coating structure was constructed by spraying aluminum nitride (AlN) particles on the surface of silicone rubber. A multiscale rough structure surface with excellent superhydrophobicity was obtained. Some people have also used natural superhydrophobic materials, such as lotus leaves [111–113], rose petals [114], etc. As shown in Figure 7B, using the lotus leaf as a template, Li et al. [112] imprinted the micro-scale pillars of the lotus leaf onto the PDMS resin. Then, the micro-scale pillar structure was transferred to the proton exchange membrane (PEM) surface by using a thermal imprinting procedure to obtain a surface with a micron structure. Finally, a secondary nano-structure was formed by using etching technology, and the surface with a multiscale nano/micro-structure was obtained.

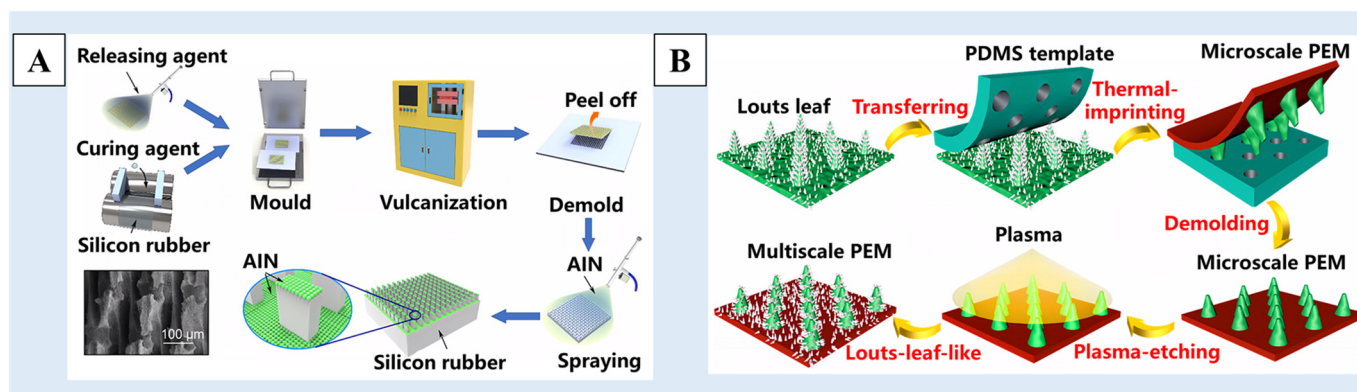


**Figure 7.** A schematic of the preparation process of (A) a multilevel rough-structured superhydrophobic surface using stainless steel mesh as a template [109] and (B) the superhydrophobic membrane with a multiscale structure using lotus leaf as a template [112]. Reprinted with permission from [109,112], Copyright 2023 American Chemical Society, Copyright 2023 American Chemical Society, respectively.

The molding method can also be applied to surfaces with complex shapes. It is relatively simple and does not require the precise control of reaction time [115,116]. The emphasis is on the quality of the molds, as a high-quality mold can produce multiple samples, enabling large-scale batch production of superhydrophobic surfaces and reducing manufacturing costs and time [106,117,118]. Nonetheless, the high cost of mold preparation and the risk of damaging surface micro-structures during the mold–material separation process, coupled with the insufficient precision of most mold fabrication methods, pose challenge in achieving a one-step formation of nano/micro-structured multiscale superhydrophobic surfaces. We still need other methods to enrich the nano-structure of the surface produced by molding.

#### 2.4. Deposition Methods

There are many deposition methods for preparing superhydrophobic surfaces with multiscale structures, among which physical vapor deposition (PVD), chemical vapor deposition (CVD) and electrochemical deposition (ECD) can be used to construct structures on non-metallic surfaces [50,119,120]. When the superhydrophobic modification is carried out by using deposition methods, two steps are generally needed: one is the design of the surface nano/micro-structure; the other is the modification by low-surface-energy substances.

#### 2.4.1. Physical Vapor Deposition (PVD)

PVD is a process in which solid materials are atomized or vaporized, and deposited on the substrate surface to form thin films with thicknesses ranging from atomic layers to several micrometers [121,122]. PVD processes are often conducted in a vacuum, plasma or electrolytic environment, which can minimize gas contamination during the deposition process. In accordance with the deposition steps, Li et al. [123] employed a plasma spray system to deposit Samaria-doped ceria (SDC) at a low pressure on a ceramic substrate. And the surface was secondarily modified by stearic acid or 1,1,2,2-tetrahydroperfluorodecyltrimethoxysilane (FAS) (Figure 8A). Gao et al. [124] employed multiarc ion plating to prepare ultrathin titanium-based hard coatings on the substrate, which were then modified by perfluorodecyltriethoxysilane (PFDS). In both cases, multi-scale nano/micro-structured superhydrophobic surfaces with a water contact angle of 150° could be achieved (Figure 8B).

#### 2.4.2. Chemical Vapor Deposition (CVD)

The main difference between chemical vapor deposition, chemical bath deposition and electrochemical deposition is the different environment in which the chemical reaction takes place. CVD mainly uses one or several vapor compounds or elements containing thin-film elements to chemically react together on the surface of substrate to produce a thin film [45,125]. Commonly used deposition materials include carbon nanotubes [126,127], SiO<sub>2</sub> [128,129], TiO<sub>2</sub> [130], PDMS [131,132] and so on. For example, Tombesi et al. [133] used aerosol-assisted chemical vapor deposition (AACVD) to fabricate SiO<sub>2</sub> nano-particle films with dual-scale roughness on glass substrates. The films had excellent superhydrophobicity and transparency.

#### 2.4.3. Electrochemical Deposition (ECD)

Electrochemical deposition is a coating technology in which a redox reaction occurs under the action of an applied electric field [120,134]. Therefore, the deposited surface needs to have a certain conductivity, and carbon-based materials and silicon-based materials are usually used as substrates for electrochemical deposition in the field of non-metals. For example, Xie et al. [135], after hydrophilic treatment of the carbon cloth surface, deposited a polypyrrole nano-wire array on the surface through electrochemical deposition, carbonized it at a high temperature and finally modified it with 1H,1H,2H,2H-perfluorodecyltrimethoxysilane (FAS-17) with a low surface energy to obtain a superhydrophobic photothermal carbon-based material with a cascade nano/micro-structure (Figure 8C). When a silicon-based material is used as the substrate, the surface oxide layer needs to be removed in order to ensure the conductive effect. Using methanol as a carbon source, graphene-doped metal cobalt [136] or metal nickel [137] was used for electrochemical deposition on the surface of silicon to obtain doped graphene/metal carbon films (Figure 8D). Under SEM, it was observed that graphene and metal combined to form a nano- and multiscale composite interface, thus forming a well-structured nano/micro-structure.

The deposition method for preparing multiscale nano/micro-structured superhydrophobic surfaces is simple, reproducible, cost-effective and well developed [44,138]. It does not require complex equipment and is more suitable for large-area surface treatment [50,120,139]. Moreover, compared to the sol-gel method, it is easier to control the surface morphology. But the deposition method is constrained by the substrate surface. For example, electrochemical deposition is only applicable to conductive non-metallic materials, and its durability is inferior to etching methods.

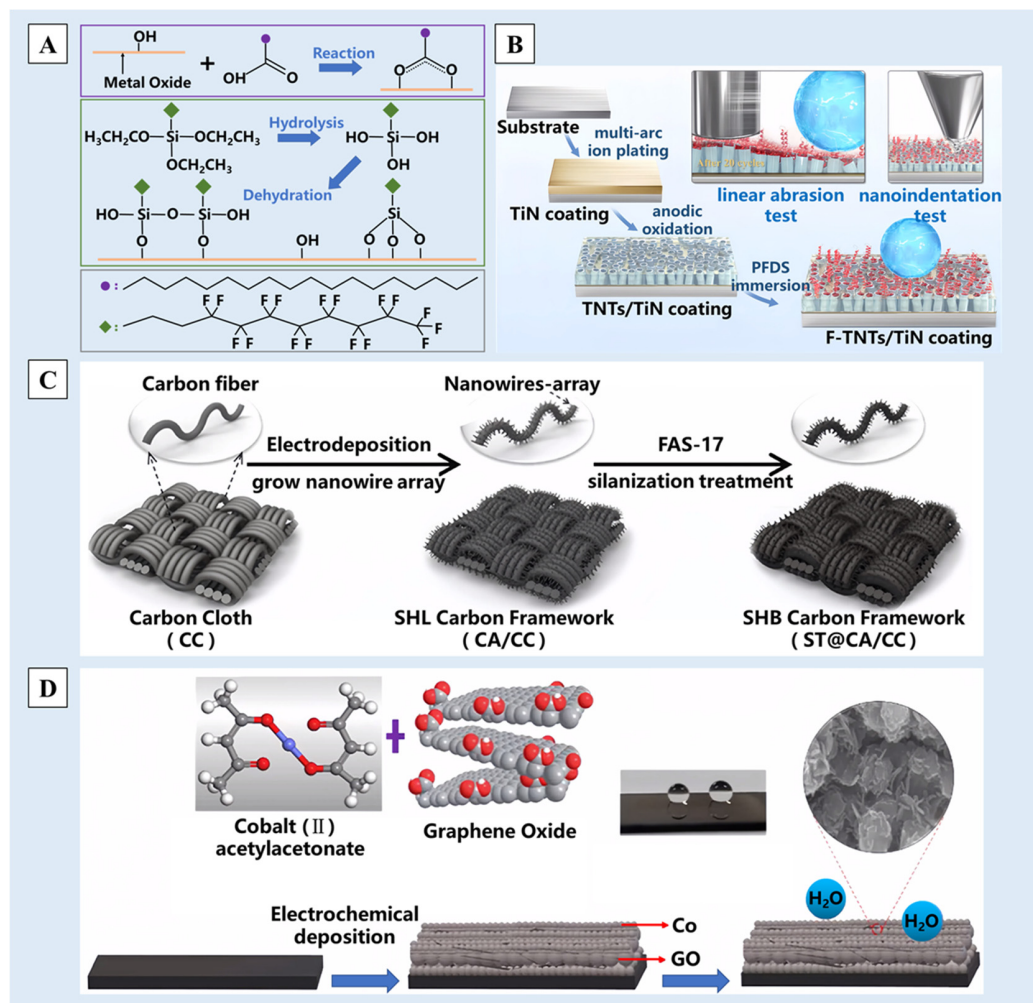


**Figure 8.** A schematic diagram of the preparation process of (A) the self-assembled films on the SDC coating surface by using stearic acid and FAS in the PVD method [123], (B) the preparation of an F-TNTs/TiN composite coating by using the PVD method [124], (C) the preparation of photothermal superhydrophobic materials by using the ECD method [135] and (D) the preparation of the superhydrophobic G-Co/a-C:H film by using the ECD method [136]. Reprinted with permission from [123,124,135,136], Copyright 2017 Springer Nature, Copyright 2023 Elsevier, Copyright 2021 American Chemical Society, Copyright 2018 John Wiley and Sons, respectively.

### 2.5. Other Methods

In addition to the above-discussed sol-gel method, molding method, etching method and deposition method, there are some other methods that can prepare multiscale-structured superhydrophobic surfaces of non-metallic materials, such as the electrospinning method [140–145], the self-assembly method [146–150], the spraying method [151–153], the dip-coating method [154,155] and so on. As shown in Figure 9A, Gan et al. [140] used a sequential electrospinning and electro spraying method to fabricate composite membranes of polystyrene-block-poly (ethylene-co-butylene)-block-polystyrene (SEBS) and fluorinated polyhedral oligomeric silsesquioxane-block-polystyrene (FPOSS-PS). The composite membranes with hierarchical geometries and low-surface-energy modifications had excellent superhydrophobicity, flush resistance and anti-adhesion properties.

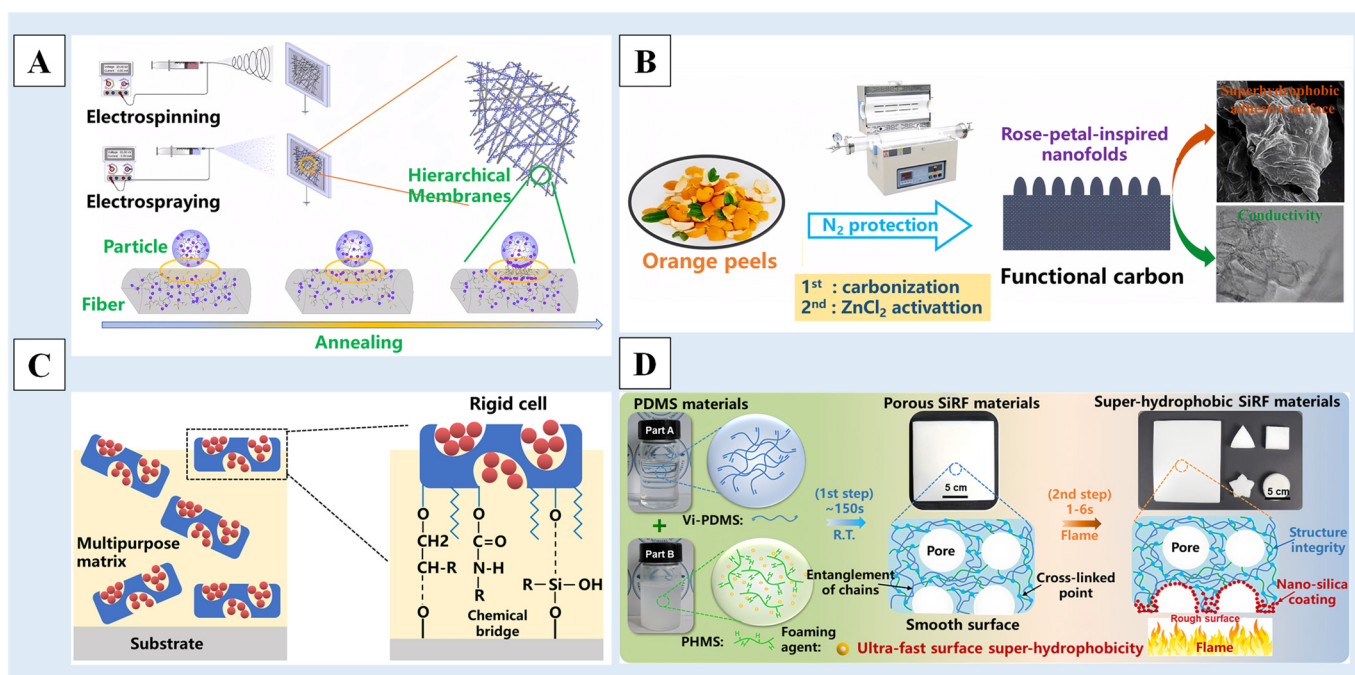


**Figure 9.** A schematic diagram of (A) the preparation of hierarchical composite membranes by using sequential electrospinning and electrospinning [140], (B) the conversion of orange peels to the conductive and superhydrophobic carbon [156], (C) the cellular design [157] and (D) the preparation process of superhydrophobic SiRF materials [158]. Reprinted with permission from [140,156–158], Copyright 2020 Elsevier, Copyright 2023 Elsevier, Copyright 2023 Springer Nature, Copyright 2021 American Chemical Society, respectively.

In addition, there are some newly invented methods as well. Chen et al. [156] pressed orange peel into a powder after drying, carbonization at a high temperature, mixing with zinc chloride, grinding and treatment at a high temperature to obtain superhydrophobic/superoleophilic carbon derived from orange peel, which has a layered structure with a nano-fold surface and an ordered graphene layer, and has excellent electrical conductivity and excellent oil–water separation characteristics (Figure 9B). Gu et al. [157] proposed a cell composed of hard porous diatomite micro-shells and releasable nano-seeds, which can simultaneously confer the multiphase repulsion and ultralong effectiveness of superhydrophobic coatings without requiring a complex structure and manufacturing process (Figure 9C). Zhang et al. [158] created a mechanically strong and superhydrophobic surface on PDMS foam by using a flame-induced pyrolysis (FIP) strategy. It only took 1–6s in the ultrafast FIP process to build a strong special wavy rough nano/micro-structure on the surface of the silicone rubber foam (SiRF) material to achieve superhydrophobic surface characteristics (Figure 9D).

### 3. Application

The technology of multiscale superhydrophobic modification of non-metallic surfaces is rapidly gaining prominence, and researchers are making unremitting efforts to achieve innovative applications in various fields, including architecture, transportation, healthcare and energy. Here, we summarize several representative applications of nano/micro-multiscale superhydrophobic modifications of non-metallic surfaces, including pollution-resistant, self-cleaning, microfluidics and anti-icing applications, which can demonstrate its importance and widespread applicability across multiple fields, and offer readers a comprehensive view of this technology for a better understanding [49,50,120,159–161].

### 3.1. Anti-Icing

Ice accretion on surfaces tends to cause equipment overload and operational damage. Furthermore, the excessive accumulation of ice, followed by the shedding of ice, may result in abnormal service conditions, potentially causing severe safety incidents and economic losses [162]. These disasters occur in numerous fields, such as aviation, power production, building construction and transportation [163–167]. In view of these security risks and energy waste issues, the superhydrophobic modification of material surfaces has become a potential solution to anti-icing issues in recent years [168,169]. The characteristics of a low surface energy, high contact angle and low roll-off angle exhibited by superhydrophobic surfaces can effectively prevent the condensation of water vapor from the air on the surface of equipment and expedite the rolling of water droplets, thereby preventing or delaying icing [163,170,171].

The icing time and ice adhesion strength are two important indicators for evaluating the anti-icing performance of superhydrophobic surfaces [172]. Numerous studies have confirmed that non-metallic superhydrophobic surfaces with nano/micro-structures can prolong the icing time and reduce the ice adhesion strength [173,174], and superhydrophobic surfaces with different nano/micro-sizes exhibit varying delaying effects on icing time [175]. He et al. [109] prepared a multiscale superhydrophobic surface on rubber by using the molding method, and the icing time increased by 3.6 times at  $-10\text{ }^{\circ}\text{C}$ , as is shown in Figure 10A. Treating carbon fiber-reinforced polymer (CFRP) and polymethyl methacrylate (PMMA) with laser etching could also produce superhydrophobic surfaces with nano/micro-structures, and the test results of icing delay time further support that superhydrophobic surfaces can extend the ice formation time by more than three times [176–178]. Wang et al. [179] also prepared a superhydrophobic coating on glass slides by using the spraying method, reducing the ice adhesion strength from  $1473 \pm 74\text{ kPa}$  for the substrate to  $194\text{ kPa}$  for the coating, which can be tested by the device depicted in Figure 10B.

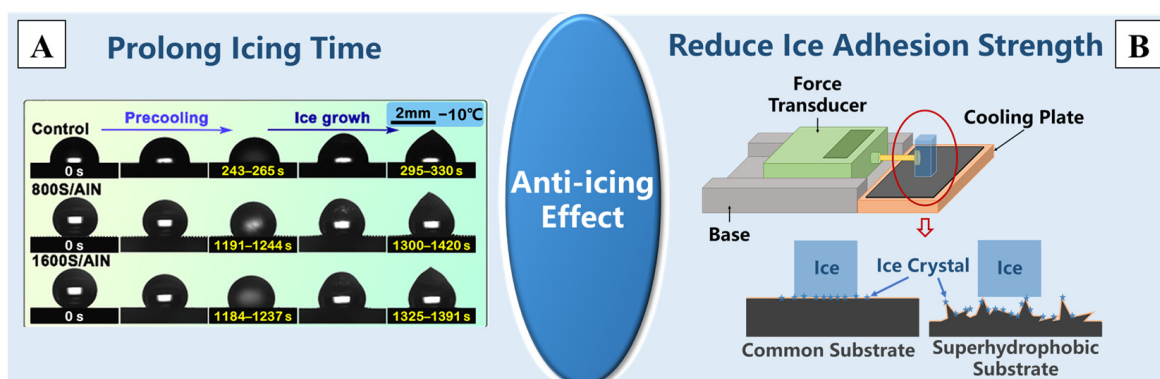


**Figure 10.** The two aspects of the improvement in the anti-icing effect due to superhydrophobic modification: (A) the prolongation of the icing time [109] and (B) the reduction in the ice adhesion strength [173,174]. Reprinted with permission from [109,173,174], Copyright 2023 American Chemical Society, Copyright 2021 Springer Nature, Copyright 2019 Elsevier, respectively.

Usually, multiscale superhydrophobic surfaces are combined with other anti-icing or de-icing methods to further enhance the capability of ice prevention, such as the photothermal method [135,180–182] and the electrothermal method [155,183]. When combined with thermal methods, the superhydrophobic layer can remain unfrozen for a long time at a low temperature or cause the ice layer to melt into liquid and rapidly detach in order to prevent recondensation.

### 3.2. Water–Oil Separation

With the rapid development of the energy industry and catering industry, more and more waste oil is produced and discharged into water, resulting in many environmental and water issues [184–186]. By adjusting the nano/micro-structure of non-metallic surfaces to create different contact angles with water and oil, efficient water–oil separation can be achieved [1]. The principle of water–oil separation through the use of superhydrophobic materials and a comparison of the contact angle are shown in Figure 11.

Different non-metallic multiscale superhydrophobic materials have been proposed and applied for water–oil separation. Fabrics have a micro-fiber structure, which helps in the formation of small pores and channels for liquid [187]. They are also environmentally friendly and reasonably priced. If the surface undergoes superhydrophobic modification, they are highly suitable as a filtration material for water–oil separation [188–190]. Polylactic acid (PLA) is a degradable and environmentally friendly material that can be directly loaded or grown with nano-structures on non-woven fabric made of PLA [191,192]. Coating PLA nanospheres mixed with dioxane on non-woven fabric [193] can also impart excellent hydrophobic and oleophilic properties, completing the water–oil separation process. Other processing methods, such as functionalizing polyacrylonitrile (PAN) non-woven fabric (NWF) with iron hydroxide nano-particles and the in situ deposition of the iron palmitate complex nano/micro-particles, can achieve a water–oil separation efficiency very close to 100% based on the multiscale nano/micro-structures [194]. These validate the potential application of superhydrophobic fabric with multiscale nano/micro-structures in the field of water–oil separation. Polymer membranes [195] and SiC membranes [196,197] can also satisfy the necessary requirements. By using the molding method or the deposition method, the surface can be endowed with nano/micro-structures, exhibiting excellent water–oil separation efficiency. Interestingly, materials commonly found in daily life with loose and porous structures, such as orange peels [156] and cigarette filters [198], can be potential choices for preparing water–oil separation materials.

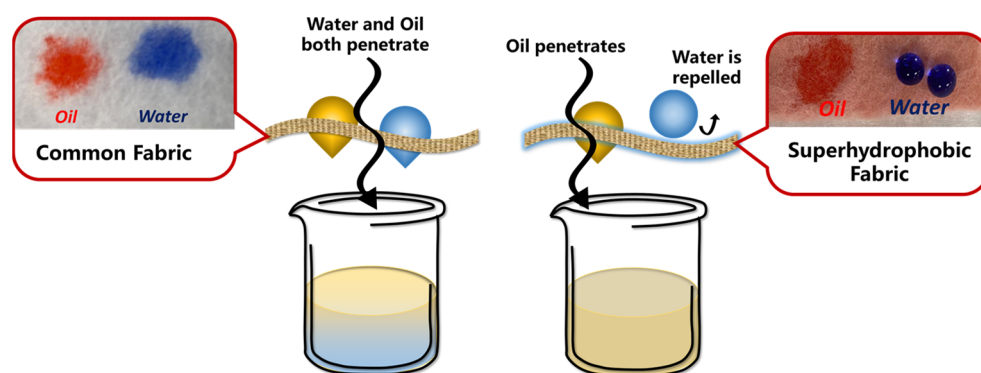


**Figure 11.** The principle and experimental results of water–oil separation by using superhydrophobic fibers [194] (reproduced from [194] with permission (2022) of the American Chemical Society).

### 3.3. Anti-Fog

Fogging commonly arises when humid air encounters surfaces or equipment with a lower temperature [199]. For surfaces such as glass or transparent polymers, fogging will reduce light transmission and have adverse effects on daily life and industrial production [200]. Superhydrophobic modification of transparent surfaces, which can achieve anti-fogging, plays a vital role in the areas where it is needed, reducing the impact of surface liquids on performance.

Transparent surfaces modified with different materials to form nano/micro-structures for anti-fogging have been widely researched in the past few decades. Nano-sized titanium dioxide [201] or silicon dioxide [26,202] are both good choices as surface modification materials, as they both have a certain degree of light transmission. For example, by loading

2–3 nm titanium dioxide particles onto silica micro-particles, a robust transparent coating with good anti-fogging properties can be prepared [203], as is shown in Figure 12A, and it also has excellent self-cleaning properties. With the help of mold imprinting [204] or laser pulse deposition [205], multiscale titanium dioxide structures can be created on transparent surfaces, endowing the coating with excellent superhydrophobic properties while maintaining a light transmittance of over 90% by adjusting the spacing of the nano/micro-structure, achieving a transparent surface with anti-fogging functions. Other materials like bio-inspired ZnO micro-spheres [25] or ZnO nano-particles [206] can also be employed for surface modification to achieve an exceptional light transparency and anti-fog performance of transparent superhydrophobic surfaces.

It should be mentioned that employing etching or molding methods can endow the transparent materials' own surface with superhydrophobicity. For example, it was reported that a method combining colloidal lithography and self-assembly engineered hierarchical conical structures achieved superhydrophobicity, which provided a WCA of  $175.3^\circ$  and low contact angle hysteresis ( $2.7^\circ$ ) [207]. Figure 12B illustrates the anti-fog performance of this surface, showing that even under high-humidity conditions, the text below remains clearly visible compared to the untreated surface. Solidifying the transparent materials on molds with multiscale nano/micro-structures, directly forming films with superhydrophobic properties, can also achieve surfaces with an excellent anti-fog performance [208,209]. A previous report demonstrates that UV-curable polymers can be initially cured into a film on a transparent surface and then treated by multiple curing steps to generate nano/micro-level roughness, achieving superhydrophobicity with a contact angle of  $172^\circ$ . Lenses treated by such materials, as shown in Figure 12C, can still maintain good transparency in high-temperature water vapor environments, showing excellent anti-fog properties [210].

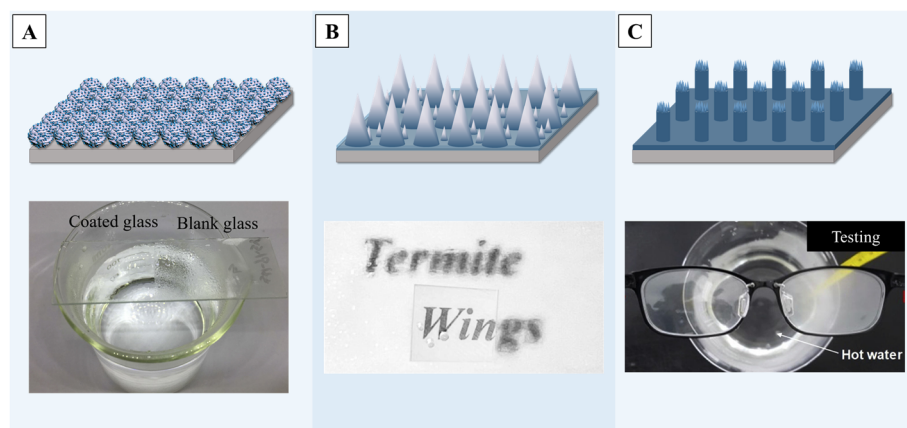


**Figure 12.** (A) Multifunctional nano-coatings of dendritic porous silica nano-particles (DPSNs) @X% TiO<sub>2</sub> with tunable sizes of TiO<sub>2</sub> nano-particles (NPs), with the outcome of an enhanced anti-fogging property [203]. (B) An illustration of the fabrication procedure for combining colloidal lithography and self-assembly engineered hierarchical conical structures and the performance of anti-fogging [207]. (C) The results of hierarchical superhydrophobic polymer (HSP) films fabricated by using photopatterning with a sandpaper template, and the results of anti-fogging tests [210]. Reprinted with permission from [203,207,210], Copyright 2020 Elsevier, Copyright 2023 Elsevier, Copyright 2019 Elsevier, respectively.

### 3.4. Self-Cleaning

There is an old saying in China which is as follows: “Lotus unsullied from mud, wash clean without demon”. A surface which has self-cleaning properties can clean its surface itself without any external source, while superhydrophobic surfaces provide a self-cleaning function for pollutants due to its low roll-off angle [59,211–214]. Briefly, self-cleaning is achieved through the combination of rainwater and a specific tilt angle when there is dust, microorganisms and other stains deposited on the surface of a superhydrophobic coating.

In the laboratory, the self-cleaning process can be simulated by dripping water onto the inclined sample surface, as shown in Figure 13A. Such self-cleaning superhydrophobic surfaces find versatile applications in daily life, including car windshields, windows, glass doors, skyscrapers, solar panels, fabrics, sports shoes, metals, paper, sponges, wood, marble and so on [160,215]. It was reported that a superhydrophobic self-cleaning surface based on two types of silica nano-particles with distinct morphologies can remove the fluorescent particles accumulated on the surface due to rolling water droplets [216], as shown in Figure 13B. Constructing multiscale structures on fabrics can also help to achieve self-cleaning functionalization, which can reduce detergent waste, time and labor [217,218]. Pakdel et al. [219] used TiO<sub>2</sub> particles in the hydrothermal method, followed by nitrogen doping to obtain N-doped TiO<sub>2</sub>, which resulted in flower-like structures on the surface. Through a facile dip-coating method, the particles composed of PDMS were applied on the cotton fabric, forming a nano/micro-structure with commendable self-cleaning properties, as illustrated by Figure 13C.

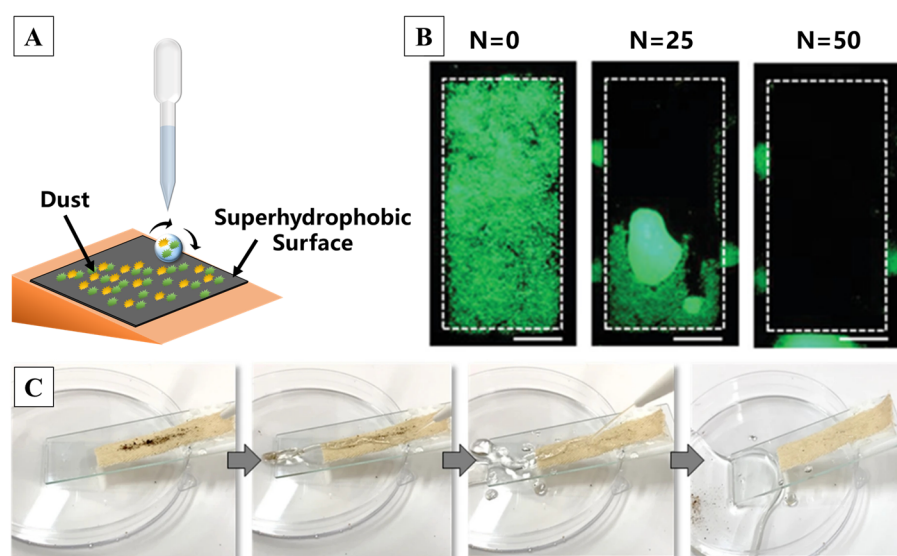


**Figure 13.** (A) A schematic diagram of the self-cleaning test setup [216]. (B,C) A quantitative and qualitative demonstration of superhydrophobic surface self-cleaning capabilities [216,219], respectively. (N is the number of droplets. Scale bars: 1 cm.) Reprinted with permission from [216,219], Copyright 2022 John Wiley and Sons, Copyright 2021 Springer Nature, respectively.

### 3.5. Other Applications

Due to the diverse types and wide range of applications of non-metallic materials, in addition to the four main directions mentioned above, superhydrophobic non-metallic surfaces can also be used in other applications such as microfluidics, food packaging, stain resistance [220], UV resistance [67,221] and so on, with the experimental results of these applications shown sequentially in Figure 14.

In the field of microfluidics, micro-droplets have important applications in areas such as drug release, virus detection and catalysts due to their small volume, large surface area, fast speed, high throughput, and uniform size [222,223]. Superhydrophobic surfaces, with their extremely small roll-off angles, can achieve efficient manipulation of droplets by designing a directional superhydrophobic surface so that the droplet can have a small roll-off angle in a specific direction [92,224], or by adjusting the contact angles at specific locations on the surface to make the droplet come into contact with the surface at selected positions [225].

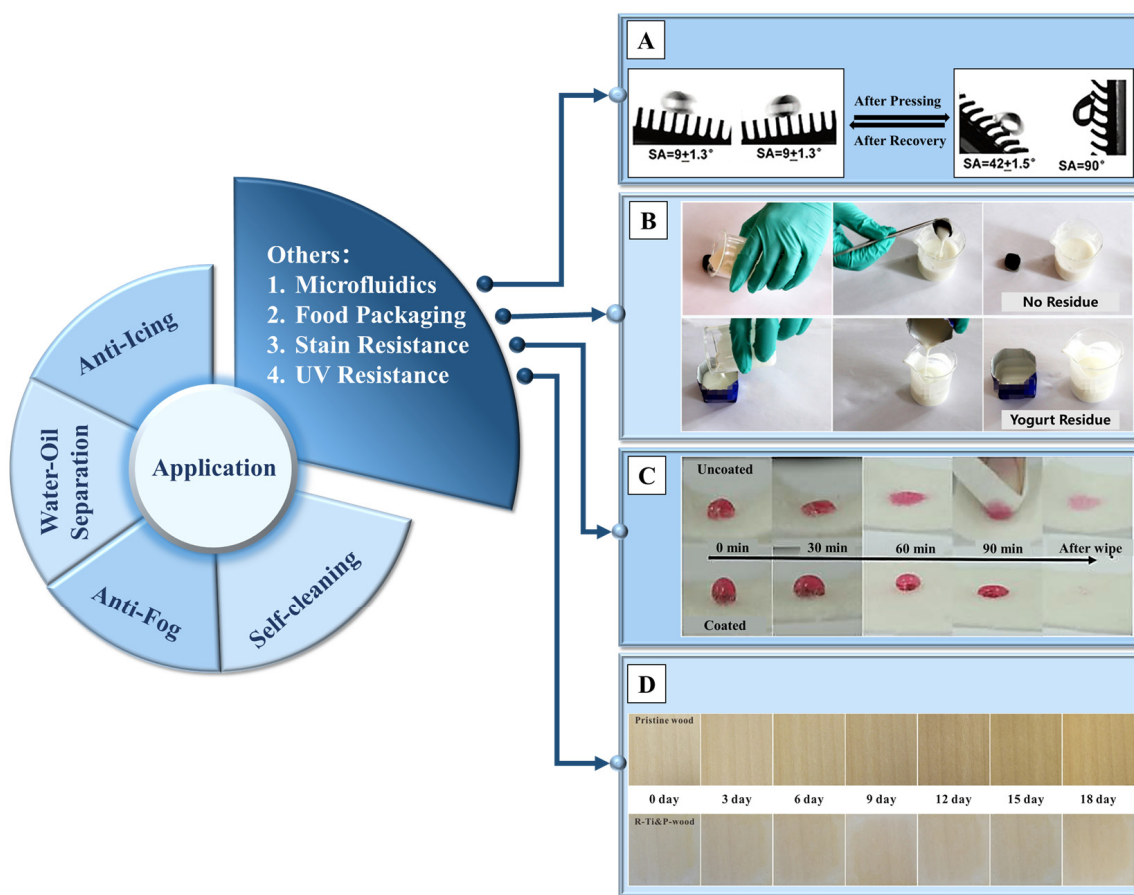


**Figure 14.** A summary of the non-metallic superhydrophobic surface, with the test result of (A) controlling the micro-liquid flow direction due to the directional superhydrophobic surface [224]; (B) the residue of yogurt after pouring, compared with commercial packaging [86]; (C) the stain resistance of pristine and silica nanoparticle-coated cashmere fabrics [220]; and (D) the pristine wood and coated wood within 18 days (taken every 3 days) after UV irradiation [67]. Reprinted with permission from [67,86,220,224]. Copyright 2021 Springer Nature, Copyright 2021 Springer Nature, Copyright 2020 Elsevier, Copyright 2020 American Chemical Society, respectively.

In the field of food packaging, such as milk containers, residue inside the container during pouring will lead to food waste. Edible wax materials are treated and sprayed on the surface of elastic films, presenting a multiscale structure with wrinkles, resulting in extremely high contact angles for common beverages such as cola, milk and juice [226]. Beyond that, using magnetic particles to form a multiscale nano/micro-structured conical array on the surface of PDMS, with edible wax vapor sprayed on it, can achieve complete pouring of yogurt inside the container [86].

#### 4. Conclusions

This paper offers a comprehensive summary of recent research on superhydrophobic modification of non-metallic material surfaces using multiscale nano/micro-structures. It mainly introduces various preparation methods, including the sol-gel method, molding method, etching method, deposition method, etc. Moreover, a summary is provided for the basic principles, preparation processes, research status, and advantages and disadvantages of these methods. It also shows the practical applications of superhydrophobic modification of non-metallic surfaces, such as anti-icing, oil-water separation, self-cleaning, etc. All of these have excellent application prospects by utilizing the performance advantages of superhydrophobicity according to specific needs.

Although superhydrophobic surfaces with multiscale nano/micro-structures have better durability than those with single-level nano-structures, the performance may decline over time, especially when encountering harsh environments such as dusty weather, extremely low temperatures and high-humidity conditions. Moreover, the preparation of multiscale nano/micro-structured surfaces generally requires multiple steps, posing challenges for the reproducibility of the process, and consequently hindering future large-scale applications in the engineering field. Hence, future key research priorities of non-metallic multiscale superhydrophobic surfaces for practical applications should focus on material designs with high durability and preparation techniques that are easy, easily scalable, effective and cost-efficient. The prospect of the preparation of multiscale nano/micro-structures also involves the integration of multiple disciplines, including materials science, nano-technology, surface science and other fields, which will provide us with a deeper understanding and means to control the surface properties of materials. This will allow non-metallic materials to play a more important role in scientific research and industrial applications, laying a solid foundation for future technology and innovation.

**Author Contributions:** Q.G., J.M., T.Y., H.J., J.Z. and H.G. wrote and edited the manuscript from an original draft produced by Q.G. and J.M. Q.G. and J.M. contributed equally to this work. All authors have read and agreed to the published version of the manuscript.

**Funding:** This research received no external funding.

**Conflicts of Interest:** The authors declare no conflicts of interest.

## References

1. Qiu, L.; Sun, Y.; Guo, Z. Designing novel superwetting surfaces for high-efficiency oil–water separation: Design principles, opportunities, trends and challenges. *J. Mater. Chem. A* **2020**, *8*, 16831–16853. [[CrossRef](#)]
2. Si, Y.; Guo, Z. Bio-inspired writable multifunctional recycled paper with outer and inner uniform superhydrophobicity. *RSC Adv.* **2016**, *6*, 30776–30784. [[CrossRef](#)]
3. Son, T.; Yang, E.; Yu, E.; Oh, K.H.; Moon, M.-W.; Kim, H.-Y. Effects of surface nanostructures on self-cleaning and anti-fogging characteristics of transparent glass. *J. Mech. Sci. Technol.* **2017**, *31*, 5407–5414. [[CrossRef](#)]
4. Hwang, J.; Ahn, Y. Fabrication of Superhydrophobic Silica Nanoparticles and Nanocomposite Coating on Glass Surfaces. *Bull. Korean Chem. Soc.* **2015**, *36*, 391–394. [[CrossRef](#)]
5. Ren, S.; Chen, Y.; Xu, K.; Liu, J.; Sun, J.; Zhao, D.; Ling, S.; Song, J.; Hua, S. Maintenance of superhydrophobic concrete for high compressive strength. *J. Mater. Sci.* **2021**, *56*, 4588–4598. [[CrossRef](#)]
6. Zhu, J.; Liao, K. A facile and low-cost method for preparing robust superhydrophobic cement block. *Mater. Chem. Phys.* **2020**, *250*, 123064. [[CrossRef](#)]
7. Dai, Z.; Guo, H.; Huang, Q.; Ding, S.; Liu, Y.; Gao, Y.; Zhou, Y.; Sun, G.; Zhou, B. Mechanically robust and superhydrophobic concrete based on sacrificial template approach. *Cem. Concr. Compos.* **2022**, *134*, 104796. [[CrossRef](#)]
8. Singh, A.K. Surface engineering using PDMS and functionalized nanoparticles for superhydrophobic coatings: Selective liquid repellence and tackling COVID-19. *Prog. Org. Coat.* **2022**, *171*, 107061. [[CrossRef](#)]
9. Gong, B.; Ma, L.; Guan, Q.; Tan, R.; Wang, C.; Wang, Z.; Wang, K.; Liu, C.; Deng, C.; Song, W.; et al. Preparation and particle size effects study of sustainable self-cleaning and durable silicon materials with superhydrophobic surface performance. *J. Environ. Chem. Eng.* **2022**, *10*, 107884. [[CrossRef](#)]
10. Tian, N.; Xu, D.; Wei, J.; Li, B.; Zhang, J. Long-lasting anti-bacterial face masks enabled by combining anti-bacterial materials and superhydrophobic coating. *Surf. Coat. Technol.* **2024**, *476*, 130229. [[CrossRef](#)]
11. Popova, A.A.; Dietrich, S.; Huber, W.; Reischl, M.; Peravali, R.; Levkin, P.A. Miniaturized Drug Sensitivity and Resistance Test on Patient-Derived Cells Using Droplet-Microarray. *SLAS Technol.* **2021**, *26*, 274–286. [[CrossRef](#)] [[PubMed](#)]
12. Ge, H.; Liu, Y.; Liu, F. Up to Date Review of Nature-Inspired Superhydrophobic Textiles: Fabrication and Applications. *Materials* **2023**, *16*, 7015. [[CrossRef](#)] [[PubMed](#)]
13. Jialiangkang; Xiang, F.; He, X.; Li, Z. Preparation of robust silicone superhydrophobic and antibacterial textiles using the Pickering emulsion method. *Carbohydr. Polym.* **2024**, *323*, 121419. [[CrossRef](#)] [[PubMed](#)]
14. Liu, J.; Sun, Y.; Ma, R.; Zhou, X.; Ye, L.; Mailänder, V.; Steffen, W.; Kappl, M.; Butt, H.-J. Mechanically Robust and Flame-Retardant Superhydrophobic Textiles with Anti-Biofouling Performance. *Langmuir* **2022**, *38*, 12961–12967. [[CrossRef](#)] [[PubMed](#)]
15. Wang, G.; Li, A.; Zhao, W.; Xu, Z.; Ma, Y.; Zhang, F.; Zhang, Y.; Zhou, J.; He, Q. A Review on Fabrication Methods and Research Progress of Superhydrophobic Silicone Rubber Materials. *Adv. Mater. Interfaces* **2021**, *8*, 2001460. [[CrossRef](#)]
16. Jeevahan, J.; Chandrasekaran, M.; Britto Joseph, G.; Durairaj, R.B.; Mageshwaran, G. Superhydrophobic surfaces: A review on fundamentals, applications, and challenges. *J. Coat. Technol. Res.* **2018**, *15*, 231–250. [[CrossRef](#)]

17. Lv, J.; Yue, Q.-x.; Ding, R.; Wang, X.; Gui, T.-j.; Zhao, X.-d. The Application of Electrochemical Noise for the Study of Metal Corrosion and Organic Anticorrosion Coatings: A Review. *ChemElectroChem* **2021**, *8*, 337–351. [CrossRef]
18. Ghunem, R.A.; Cherney, E.A.; Farzaneh, M.; Momen, G.; Illias, H.A.; Malagón, G.A.M.; Peesapati, V.; Yin, F. Development and Application of Superhydrophobic Outdoor Insulation: A Review. *IEEE Trans. Dielectr. Electr. Insul.* **2022**, *29*, 1392–1399. [CrossRef]
19. Li, C.; Li, N.; Zhang, X.; Dong, Z.; Chen, H.; Jiang, L. Uni-Directional Transportation on Peristome-Mimetic Surfaces for Completely Wetting Liquids. *Angew. Chem. Int. Ed.* **2016**, *55*, 14988–14992. [CrossRef]
20. Feng, X.-Q.; Gao, X.; Wu, Z.; Jiang, L.; Zheng, Q.-S. Superior Water Repellency of Water Strider Legs with Hierarchical Structures: Experiments and Analysis. *Langmuir* **2007**, *23*, 4892–4896. [CrossRef]
21. Feng, L.; Zhang, Y.; Xi, J.; Zhu, Y.; Wang, N.; Xia, F.; Jiang, L. Petal Effect: A Superhydrophobic State with High Adhesive Force. *Langmuir* **2008**, *24*, 4114–4119. [CrossRef] [PubMed]
22. Guo, Z.; Liu, W. Biomimic from the superhydrophobic plant leaves in nature: Binary structure and unitary structure. *Plant Sci.* **2007**, *172*, 1103–1112. [CrossRef]
23. Wang, P.; Zhao, H.; Zheng, B.; Guan, X.; Sun, B.; Liao, Y.; Yue, Y.; Duan, W.; Ding, H. A Super-robust Armoured Superhydrophobic Surface with Excellent Anti-icing Ability. *J. Bionic Eng.* **2023**, *20*, 1891–1904. [CrossRef]
24. Chen, J.; Fu, C.; Li, J.; Tang, W.; Gao, X.; Zhang, J. Fabrication and Experimental Study of Micro/Sub-Micro Porous Copper Coating for Anti-Icing Application. *Materials* **2023**, *16*, 3774. [CrossRef] [PubMed]
25. Sun, Z.; Liao, T.; Liu, K.; Jiang, L.; Kim, J.H.; Dou, S.X. Fly-Eye Inspired Superhydrophobic Anti-Fogging Inorganic Nanostructures. *Small* **2014**, *10*, 3001–3006. [CrossRef] [PubMed]
26. Feng, C.; Zhang, Z.; Li, J.; Qu, Y.; Xing, D.; Gao, X.; Zhang, Z.; Wen, Y.; Ma, Y.; Ye, J.; et al. A Bioinspired, Highly Transparent Surface with Dry-Style Antifogging, Antifrosting, Antifouling, and Moisture Self-Cleaning Properties. *Macromol. Rapid Commun.* **2019**, *40*, 1800708. [CrossRef] [PubMed]
27. Mohd, G.; Majid, K.; Lone, S. Synergetic Role of Nano-/Microscale Structures of the Trifolium Leaf Surface for Self-Cleaning Properties. *Langmuir* **2023**, *39*, 6178–6187. [CrossRef]
28. Cai, H.; Duan, C.; Fu, M.; Zhang, J.; Huang, H.; Hu, Y.; Shi, J.; Ye, D. Scalable Fabrication of Superhydrophobic Coating with Rough Coral Reef-Like Structures for Efficient Self-Cleaning and Oil-Water Separation: An Experimental and Molecular Dynamics Simulation Study. *Small* **2023**, *19*, 2207118. [CrossRef] [PubMed]
29. Su, B.; Tian, Y.; Jiang, L. Bioinspired Interfaces with Superwettability: From Materials to Chemistry. *J. Am. Chem. Soc.* **2016**, *138*, 1727–1748. [CrossRef]
30. Wenzel, R.N. Resistance of solid surfaces to wetting by water. *Ind. Eng. Chem.* **1936**, *28*, 988–994. [CrossRef]
31. Cassie, A.B.D.; Baxter, S. Wettability of porous surfaces. *Trans. Faraday Soc.* **1944**, *40*, 546–551. [CrossRef]
32. Zhang, X.; Wang, L.; Levänen, E. Superhydrophobic surfaces for the reduction of bacterial adhesion. *RSC Adv.* **2013**, *3*, 12003–12020. [CrossRef]
33. Pi, P.; Hou, K.; Zhou, C.; Wen, X.; Xu, S.; Cheng, J.; Wang, S. A novel superhydrophilic-underwater superoleophobic Cu<sub>2</sub>S coated copper mesh for efficient oil-water separation. *Mater. Lett.* **2016**, *182*, 68–71. [CrossRef]
34. Cao, L.; Jones, A.K.; Sikka, V.K.; Wu, J.; Gao, D. Anti-Icing Superhydrophobic Coatings. *Langmuir* **2009**, *25*, 12444–12448. [CrossRef] [PubMed]
35. Groten, J.; Rühle, J. Surfaces with Combined Microscale and Nanoscale Structures: A Route to Mechanically Stable Superhydrophobic Surfaces? *Langmuir* **2013**, *29*, 3765–3772. [CrossRef] [PubMed]
36. Lee, E.J.; Kim, J.J.; Cho, S.O. Fabrication of Porous Hierarchical Polymer/Ceramic Composites by Electron Irradiation of Organic/Inorganic Polymers: Route to a Highly Durable, Large-Area Superhydrophobic Coating. *Langmuir* **2010**, *26*, 3024–3030. [CrossRef]
37. Jung, Y.C.; Bhushan, B. Mechanically Durable Carbon Nanotube–Composite Hierarchical Structures with Superhydrophobicity, Self-Cleaning, and Low-Drag. *ACS Nano* **2009**, *3*, 4155–4163. [CrossRef]
38. Chu, J.; Tian, G.; Feng, X. Recent advances in prevailing antifogging surfaces: Structures, materials, durability, and beyond. *Nanoscale* **2023**, *15*, 11366–11402. [CrossRef]
39. Wong, S.M.; Ho, H.W.; Abdullah, M.Z. Design and Fabrication of a Dual Rotor-Embedded Wing Vertical Take-Off and Landing Unmanned Aerial Vehicle. *Unmanned Syst.* **2020**, *09*, 45–63. [CrossRef]
40. Yan, F.; Xitao, Z.; Shuyi, W.; Zhendong, L. Layup optimization design and analysis of super lightweight composite wing. *Acta Aeronaut. Astronaut. Sin.* **2015**, *36*, 1858–1866.
41. Xiang, B.; Liu, Q.; Sun, Q.; Gong, J.; Mu, P.; Li, J. Recent advances in eco-friendly fabrics with special wettability for oil/water separation. *Chem. Commun.* **2022**, *58*, 13413–13438. [CrossRef] [PubMed]
42. Fürtauer, S.; Hassan, M.; Elsherbiny, A.; Gabal, S.A.; Mehanny, S.; Abushammala, H. Current Status of Cellulosic and Nanocellulosic Materials for Oil Spill Cleanup. *Polymers* **2021**, *13*, 2739. [CrossRef] [PubMed]
43. Wikimedia Commons. Available online: <http://wthielicke.gmxhome.de/bionik/indexuk.htm> (accessed on 6 December 2007).
44. Nguyen-Tri, P.; Tran, H.N.; Plamondon, C.O.; Tuduri, L.; Vo, D.-V.N.; Nanda, S.; Mishra, A.; Chao, H.-P.; Bajpai, A.K. Recent progress in the preparation, properties and applications of superhydrophobic nano-based coatings and surfaces: A review. *Prog. Org. Coat.* **2019**, *132*, 235–256. [CrossRef]
45. Wan, T.; Wang, B.; Han, Q.; Chen, J.; Li, B.; Wei, S. A review of superhydrophobic shape-memory polymers: Preparation, activation, and applications. *Appl. Mater. Today* **2022**, *29*, 101665. [CrossRef]

46. Ge-Zhang, S.; Yang, H.; Ni, H.; Mu, H.; Zhang, M. Biomimetic superhydrophobic metal/nonmetal surface manufactured by etching methods: A mini review. *Front. Bioeng. Biotechnol.* **2022**, *10*, 958095. [[CrossRef](#)] [[PubMed](#)]
47. Wang, J.-N.; Zhang, Y.-L.; Liu, Y.; Zheng, W.; Lee, L.P.; Sun, H.-B. Recent developments in superhydrophobic graphene and graphene-related materials: From preparation to potential applications. *Nanoscale* **2015**, *7*, 7101–7114. [[CrossRef](#)] [[PubMed](#)]
48. Feng, X.; Zhang, X.; Tian, G. Recent advances in bioinspired superhydrophobic ice-proof surfaces: Challenges and prospects. *Nanoscale* **2022**, *14*, 5960–5993. [[CrossRef](#)]
49. Zeng, Q.; Zhou, H.; Huang, J.; Guo, Z. Review on the recent development of durable superhydrophobic materials for practical applications. *Nanoscale* **2021**, *13*, 11734–11764. [[CrossRef](#)] [[PubMed](#)]
50. Wei, X.; Niu, X. Recent Advances in Superhydrophobic Surfaces and Applications on Wood. *Polymers* **2023**, *15*, 1682. [[CrossRef](#)]
51. Yang, H.; Zhu, M.; Li, Y. Sol-gel research in China: A brief history and recent research trends in synthesis of sol-gel derived materials and their applications. *J. Sol-Gel Sci. Technol.* **2022**, *106*, 406–421. [[CrossRef](#)]
52. Mohd Aref, Y.; Othaman, R.; Anuar, F.H.; Ku Ahmad, K.Z.; Baharum, A. Superhydrophobic Modification of Sansevieria trifasciata Natural Fibres: A Promising Reinforcement for Wood Plastic Composites. *Polymers* **2023**, *15*, 594. [[CrossRef](#)]
53. Chujo, Y.; Saegusa, T. Organic polymer hybrids with silica gel formed by means of the sol-gel method. *Adv. Polym. Sci.* **1992**, *100*, 11–29. [[CrossRef](#)]
54. Czyzyk, S.; Dotan, A.; Dodiuk, H.; Kenig, S. Processing effects on the kinetics morphology and properties of hybrid sol-gel superhydrophobic coatings. *Prog. Org. Coat.* **2020**, *140*, 105501. [[CrossRef](#)]
55. Taurino, R.; Cannio, M.; Boccaccini, D.N.; Messori, M.; Bondioli, F. Preliminary study on the design of superhydrophobic surface by 3D inkjet printing of a sol-gel solution. *J. Sol-Gel Sci. Technol.* **2023**, *108*, 368–376. [[CrossRef](#)]
56. Yao, X.; Kong, Z.; Yang, F.; Wu, X.; Wu, Y. Study on the Difference of Superhydrophobic Characteristics of Different Wood Furniture Substrates. *Polymers* **2023**, *15*, 1644. [[CrossRef](#)]
57. Gosiamemang, T.; Heng, J.Y.Y. Sodium hydroxide catalysed silica sol-gel synthesis: Physicochemical properties of silica nanoparticles and their post-grafting using C8 and C18 alkyl-organosilanes. *Powder Technol.* **2023**, *417*, 118237. [[CrossRef](#)]
58. Wang, Y.; Ge-Zhang, S.; Mu, P.; Wang, X.; Li, S.; Qiao, L.; Mu, H. Advances in Sol-Gel-Based Superhydrophobic Coatings for Wood: A Review. *Int. J. Mol. Sci.* **2023**, *24*, 9675. [[CrossRef](#)]
59. Latthe, S.S.; Sutar, R.S.; Kodag, V.S.; Bhosale, A.K.; Kumar, A.M.; Kumar Sadasivuni, K.; Xing, R.; Liu, S. Self-cleaning superhydrophobic coatings: Potential industrial applications. *Prog. Org. Coat.* **2019**, *128*, 52–58. [[CrossRef](#)]
60. Espanhol-Soares, M.; Costa, L.; Silva, M.R.A.; Soares Silva, F.; Ribeiro, L.M.S.; Gimenes, R. Super-hydrophobic coatings on cotton fabrics using sol-gel technique by spray. *J. Sol-Gel Sci. Technol.* **2020**, *95*, 22–33. [[CrossRef](#)]
61. Gao, X.; Wang, M.; He, Z. Superhydrophobic Wood Surfaces: Recent Developments and Future Perspectives. *Coatings* **2023**, *13*, 877. [[CrossRef](#)]
62. Zheng, K.; Zhu, J.; Liu, H.; Zhang, X.; Wang, E. Facile fabrication of superhydrophobic polymethyltriethoxysilane-polymethylhydrosiloxane coatings. *J. Dispers. Sci. Technol.* **2022**, *43*, 273–281. [[CrossRef](#)]
63. Periyasamy, A.P.; Venkataraman, M.; Kremenakova, D.; Militky, J.; Zhou, Y. Progress in Sol-Gel Technology for the Coatings of Fabrics. *Materials* **2020**, *13*, 1838. [[CrossRef](#)]
64. Xie, A.; Cui, J.; Chen, Y.; Lang, J.; Li, C.; Yan, Y.; Dai, J. One-step facile fabrication of sustainable cellulose membrane with superhydrophobicity via a sol-gel strategy for efficient oil/water separation. *Surf. Coat. Technol.* **2019**, *361*, 19–26. [[CrossRef](#)]
65. Mahadik, S.A.; Mahadik, S.S. Surface morphological and topographical analysis of multifunctional superhydrophobic sol-gel coatings. *Ceram. Int.* **2021**, *47*, 29475–29482. [[CrossRef](#)]
66. Sutar, R.S.; Gaikwad, S.S.; Latthe, S.S.; Kodag, V.S.; Deshmukh, S.B.; Saptal, L.P.; Kulal, S.R.; Bhosale, A.K. Superhydrophobic Nanocomposite Coatings of Hydrophobic Silica NPs and Poly(methyl methacrylate) with Notable Self-Cleaning Ability. *Macromol. Symp.* **2020**, *393*, 2000116. [[CrossRef](#)]
67. Li, Y.; Xiong, Z.; Zhang, M.; He, Y.; Yang, Y.; Liao, Y.; Hu, J.; Wang, M.; Wu, G. Development of highly durable superhydrophobic and UV-resistant wood by E-beam radiation curing. *Cellulose* **2021**, *28*, 11579–11593. [[CrossRef](#)]
68. Duan, Z.; Qu, L.; Hu, Z.; Liu, D.; Liu, R.; Zhang, Y.; Zheng, X.; Zhang, J.; Wang, X.; Zhao, G. Fabrication of micro-patterned ZrO<sub>2</sub>/TiO<sub>2</sub> composite surfaces with tunable super-wettability via a photosensitive sol-gel technique. *Appl. Surf. Sci.* **2020**, *529*, 147136. [[CrossRef](#)]
69. Stöber, W.; Fink, A.; Bohn, E. Controlled growth of monodisperse silica spheres in the micron size range. *J. Colloid Interface Sci.* **1968**, *26*, 62–69. [[CrossRef](#)]
70. Chen, R.; Xu, J.; Li, S.; Li, Q.; Wu, H.; He, Q.; Wang, Z.; Weng, F.; Mu, J. Multiscale-structured superhydrophobic/superoleophilic SiO<sub>2</sub> composite poly(ether sulfone) membranes with high efficiency and flux for water-in-oil emulsions separation under harsh conditions. *New J. Chem.* **2020**, *44*, 3824–3827. [[CrossRef](#)]
71. Dong, W.; Zhou, S.; Qian, F.; Li, Q.; Tang, G.; Xiang, T.; Long, H.-m.; Chun, T.; Lu, J.; Han, Y. Low-temperature silane coupling agent modified biomimetic micro/nanoscale roughness hierarchical structure superhydrophobic polyethylene terephthalate filter media. *Polym. Adv. Technol.* **2022**, *33*, 1655–1664. [[CrossRef](#)]
72. Wang, Z.; Yao, D.; He, Z.; Liu, Y.; Wang, H.; Zheng, Y. Fabrication of Durable, Chemically Stable, Self-Healing Superhydrophobic Fabrics Utilizing Gellable Fluorinated Block Copolymer for Multifunctional Applications. *ACS Appl. Mater. Interfaces* **2022**, *14*, 48106–48122. [[CrossRef](#)]

73. AlZadjali, S.; Matouk, Z.; AlShehhi, A.; Rajput, N.; Mohammedture, M.; Gutierrez, M. Simple, Scalable Route to Produce Transparent Superhydrophobic/Hydrophilic Film Surfaces. *Appl. Sci.* **2023**, *13*, 1707. [[CrossRef](#)]
74. Heiman-Burstein, D.; Dotan, A.; Dodiuk, H.; Kenig, S. Hybrid Sol–Gel Superhydrophobic Coatings Based on Alkyl Silane-Modified Nanosilica. *Polymers* **2021**, *13*, 539. [[CrossRef](#)]
75. Wang, Q.; Xiong, J.; Chen, G.; Xinping, O.; Yu, Z.; Chen, Q.; Yu, M. Facile Approach to Develop Hierarchical Roughness fiber@SiO<sub>2</sub> Blocks for Superhydrophobic Paper. *Materials* **2019**, *12*, 1393. [[CrossRef](#)]
76. Hu, Y.; Ma, X.; Bi, H.; Sun, J. Robust superhydrophobic surfaces fabricated by self-growth of TiO<sub>2</sub> particles on cured silicone rubber. *Colloids Surf. A Physicochem. Eng. Asp.* **2020**, *603*, 125227. [[CrossRef](#)]
77. Nasiri Khalil Abad, S.; Najibi Ilkhechi, N.; Adel, M.; Mozammel, M. Hierarchical architecture of a superhydrophobic Cd-Si co-doped TiO<sub>2</sub> thin film. *Appl. Surf. Sci.* **2020**, *533*, 147495. [[CrossRef](#)]
78. Luo, H.; Yang, M.; Li, D.; Wang, Q.; Zou, W.; Xu, J.; Zhao, N. Transparent Super-Repellent Surfaces with Low Haze and High Jet Impact Resistance. *ACS Appl. Mater. Interfaces* **2021**, *13*, 13813–13821. [[CrossRef](#)]
79. Wong, W.S.Y.; Stachurski, Z.H.; Nisbet, D.R.; Tricoli, A. Ultra-Durable and Transparent Self-Cleaning Surfaces by Large-Scale Self-Assembly of Hierarchical Interpenetrated Polymer Networks. *ACS Appl. Mater. Interfaces* **2016**, *8*, 13615–13623. [[CrossRef](#)]
80. Zhou, Y.; Liu, Y.; Du, F. Rational fabrication of fluorine-free, superhydrophobic, durable surface by one-step spray method. *Prog. Org. Coat.* **2023**, *174*, 107227. [[CrossRef](#)]
81. Patra, R.; Raju, K.R.C.S.; Murugan, K.; Subasri, R. Effect of heating rate on asperities pattern formed in sol-gel derived nanocomposite hydrophobic coatings. *J. Sol-Gel Sci. Technol.* **2022**, *103*, 50–61. [[CrossRef](#)]
82. Soueiti, J.; Saredine, R.; Kadiri, H.; Alhoussein, A.; Lerondel, G.; Habchi, R. A review of cost-effective black silicon fabrication techniques and applications. *Nanoscale* **2023**, *15*, 4738–4761. [[CrossRef](#)] [[PubMed](#)]
83. Zhuang, D.; Edgar, J.H. Wet etching of GaN, AlN, and SiC: A review. *Mater. Sci. Eng. R Rep.* **2005**, *48*, 1–46. [[CrossRef](#)]
84. Pakpum, C.; Pussadee, N. Deep reactive ion etching of alumina titanium carbide using chlorine-based plasma. *Surf. Coat. Technol.* **2016**, *306*, 194–199. [[CrossRef](#)]
85. Bing, W.; Wang, H.; Tian, L.; Zhao, J.; Jin, H.; Du, W.; Ren, L. Small Structure, Large Effect: Functional Surfaces Inspired by *Salvinia* Leaves. *Small Struct.* **2021**, *2*, 2100079. [[CrossRef](#)]
86. Song, Y.; Yu, Z.; Liu, Y.; Dong, L.; Ma, H. A Hierarchical Conical Array with Controlled Adhesion and Drop Bounce Ability for Reducing Residual Non-Newtonian Liquids. *J. Bionic Eng.* **2021**, *18*, 637–648. [[CrossRef](#)]
87. Yong, J.; Chen, F.; Yang, Q.; Zhang, D.; Du, G.; Si, J.; Yun, F.; Hou, X. Femtosecond Laser Weaving Superhydrophobic Patterned PDMS Surfaces with Tunable Adhesion. *J. Phys. Chem. C* **2013**, *117*, 24907–24912. [[CrossRef](#)]
88. Jiang, H.; Liu, J.; Song, Y.; Liu, Y.; Ren, L. Fabrication of biomimetic graphene films on fabric base by two-beam laser interference. *Chin. Sci. Bull.* **2018**, *64*, 1290–1295. [[CrossRef](#)]
89. Yong, J.; Yang, Q.; Chen, F.; Zhang, D.; Du, G.; Bian, H.; Si, J.; Yun, F.; Hou, X. Superhydrophobic PDMS surfaces with three-dimensional (3D) pattern-dependent controllable adhesion. *Appl. Surf. Sci.* **2014**, *288*, 579–583. [[CrossRef](#)]
90. Yong, J.; Chen, F.; Yang, Q.; Hou, X. Femtosecond laser controlled wettability of solid surfaces. *Soft Matter* **2015**, *11*, 8897–8906. [[CrossRef](#)]
91. Zhan, Y.L.; Ruan, M.; Li, W.; Li, H.; Hu, L.Y.; Ma, F.M.; Yu, Z.L.; Feng, W. Fabrication of anisotropic PTFE superhydrophobic surfaces using laser microprocessing and their self-cleaning and anti-icing behavior. *Colloids Surf. A Physicochem. Eng. Asp.* **2017**, *535*, 8–15. [[CrossRef](#)]
92. Fang, Y.; Yong, J.; Chen, F.; Huo, J.; Yang, Q.; Zhang, J.; Hou, X. Bioinspired Fabrication of Bi/Tridirectionally Anisotropic Sliding Superhydrophobic PDMS Surfaces by Femtosecond Laser. *Adv. Mater. Interfaces* **2018**, *5*, 1701245. [[CrossRef](#)]
93. Wang, W.; Lu, L.; Lu, X.; Liang, Z.; Tang, B.; Xie, Y. Laser-induced jigsaw-like graphene structure inspired by *Oxalis corniculata* Linn. leaf. *Bio-Des. Manuf.* **2022**, *5*, 700–713. [[CrossRef](#)]
94. Wang, Q.; Xu, S.; Xing, X.; Wang, N. Progress in fabrication and applications of micro/nanostructured superhydrophobic surfaces. *Surf. Innov.* **2022**, *10*, 89–110. [[CrossRef](#)]
95. Wohlfart, E.; Fernández-Blázquez, J.P.; Arzt, E.; del Campo, A. Nanofibrillar Patterns on PET: The Influence of Plasma Parameters in Surface Morphology. *Plasma Process. Polym.* **2011**, *8*, 876–884. [[CrossRef](#)]
96. Ko, T.-J.; Park, S.J.; Kim, M.-S.; Yoon, S.M.; Kim, S.J.; Oh, K.H.; Nahm, S.; Moon, M.-W. Single-step plasma-induced hierarchical structures for tunable water adhesion. *Sci. Rep.* **2020**, *10*, 874. [[CrossRef](#)] [[PubMed](#)]
97. Zhang, W.; Yao, J.; Liu, X.; Yan, R.; Xu, J. Adhesion behavior of different droplet on superhydrophobic surface of cotton fabric based on oxygen plasma etching. *J. Text. Inst.* **2022**, *114*, 790–800. [[CrossRef](#)]
98. Szczepanski, C.R.; Guittard, F.; Darmanin, T. Recent advances in the study and design of parahydrophobic surfaces: From natural examples to synthetic approaches. *Adv. Colloid Interface Sci.* **2017**, *241*, 37–61. [[CrossRef](#)]
99. Ghasemlou, M.; Daver, F.; Ivanova, E.P.; Adhikari, B. Bio-inspired sustainable and durable superhydrophobic materials: From nature to market. *J. Mater. Chem. A* **2019**, *7*, 16643–16670. [[CrossRef](#)]
100. Li, X.; Zhang, G.; Xu, X.; Zhao, G.; Liu, Y.; Yin, S. Fabrication of superhydrophobic surfaces on a glass substrate via hot embossing. *Ceram. Int.* **2023**, *49*, 26338–26347. [[CrossRef](#)]
101. Li, C.; Yang, J.; He, W.; Xiong, M.; Niu, X.; Li, X.; Yu, D.G. A Review on Fabrication and Application of Tunable Hybrid Micro–Nano Array Surfaces. *Adv. Mater. Interfaces* **2023**, *10*, 2202160. [[CrossRef](#)]

102. Nyström, D.; Lindqvist, J.; Östmark, E.; Antoni, P.; Carlmark, A.; Hult, A.; Malmström, E. Superhydrophobic and Self-Cleaning Bio-Fiber Surfaces via ATRP and Subsequent Postfunctionalization. *ACS Appl. Mater. Interfaces* **2009**, *1*, 816–823. [[CrossRef](#)] [[PubMed](#)]
103. Lv, T.; Cheng, Z.; Zhang, D.; Zhang, E.; Zhao, Q.; Liu, Y.; Jiang, L. Superhydrophobic Surface With Shape Memory Micro/Nanostructure and Its Application in Rewritable Chip for Droplet Storage. *ACS Nano* **2016**, *10*, 9379–9386. [[CrossRef](#)] [[PubMed](#)]
104. Zhang, Y.; Liu, Z.; Chen, A.; Wang, Q.; Zhang, J.; Zhao, C.; Xu, J.; Yang, W.; Peng, Y.; Zhang, Z. Fabrication of Micro-/Submicro-/Nanostructured Polypropylene/Graphene Superhydrophobic Surfaces with Extreme Dynamic Pressure Resistance Assisted by Single Hierarchically Porous Anodic Aluminum Oxide Template. *J. Phys. Chem. C* **2020**, *124*, 6197–6205. [[CrossRef](#)]
105. Choi, J.; Cho, W.; Jung, Y.S.; Kang, H.S.; Kim, H.-T. Direct Fabrication of Micro/Nano-Patterned Surfaces by Vertical-Directional Photofluidization of Azobenzene Materials. *ACS Nano* **2017**, *11*, 1320–1327. [[CrossRef](#)] [[PubMed](#)]
106. Yanagishita, T.; Sou, T.; Masuda, H. Micro-nano hierarchical pillar array structures prepared on curved surfaces by nanoimprinting using flexible molds from anodic porous alumina and their application to superhydrophobic surfaces. *RSC Adv.* **2022**, *12*, 20340–20347. [[CrossRef](#)] [[PubMed](#)]
107. Zhao, F.; Zhan, F.; Wang, L. Hybrid Topography of Lotus Leaf under Hydrostatic/Hydrodynamic Pressure. *Adv. Mater. Interfaces* **2022**, *10*, 2202044. [[CrossRef](#)]
108. Li, W.; Chan, C.-w.; Li, Z.; Siu, S.-Y.; Chen, S.; Sun, H.; Liu, Z.; Wang, Y.; Hu, C.; Pugno, N.M.; et al. All-perfluoropolymer, nonlinear stability-assisted monolithic surface combines topology-specific superwettability with ultradurability. *Innovation* **2023**, *4*, 100389. [[CrossRef](#)] [[PubMed](#)]
109. He, Q.; Ma, Y.; Wang, X.; Jia, Y.; Li, K.; Li, A. Superhydrophobic Flexible Silicone Rubber with Stable Performance, Anti-Icing, and Multilevel Rough Structure. *ACS Appl. Polym. Mater.* **2023**, *5*, 4729–4737. [[CrossRef](#)]
110. Gu, D.; Song, K.; Chen, S.; Liu, S.; Yang, B.; Ma, X.; Wang, Z.; Wang, S. Multistage textured superhydrophobic polytetrafluoroethylene surface prepared by fabric embossing and thermal annealing. *Mater. Lett.* **2020**, *268*, 127556. [[CrossRef](#)]
111. Wang, Y.K.; Liu, Y.P.; Li, J.; Chen, L.W.; Huang, S.L.; Tian, X.L. Fast self-healing superhydrophobic surfaces enabled by biomimetic wax regeneration. *Chem. Eng. J.* **2020**, *390*, 124311. [[CrossRef](#)]
112. Li, Y.; Wen, Q.; Zou, S.; Dan, X.; Ning, F.; Li, W.; Xu, P.; He, C.; Shen, M.; He, L.; et al. Multiscale Architected Nafion Membrane Derived from Lotus Leaf for Fuel Cell Applications. *ACS Appl. Mater. Interfaces* **2023**, *15*, 29084–29093. [[CrossRef](#)]
113. Ghasemlou, M.; Le, P.H.; Daver, F.; Murdoch, B.J.; Ivanova, E.P.; Adhikari, B. Robust and Eco-Friendly Superhydrophobic Starch Nanohybrid Materials with Engineered Lotus Leaf Mimetic Multiscale Hierarchical Structures. *ACS Appl. Mater. Interfaces* **2021**, *13*, 36558–36573. [[CrossRef](#)] [[PubMed](#)]
114. Yang, Y.; He, H.; Li, Y.; Qiu, J. Using Nanoimprint Lithography to Create Robust, Buoyant, Superhydrophobic PVB/SiO<sub>2</sub> Coatings on wood Surfaces Inspired by Red roses petal. *Sci. Rep.* **2019**, *9*, 9961. [[CrossRef](#)] [[PubMed](#)]
115. Maghsoudi, K.; Vazirinasab, E.; Momen, G.; Jafari, R. Advances in the Fabrication of Superhydrophobic Polymeric Surfaces by Polymer Molding Processes. *Ind. Eng. Chem. Res.* **2020**, *59*, 9343–9363. [[CrossRef](#)]
116. Kang, B.; Sung, J.; So, H. Realization of Superhydrophobic Surfaces Based on Three-Dimensional Printing Technology. *Int. J. Precis. Eng. Manuf.-Green Technol.* **2019**, *8*, 47–55. [[CrossRef](#)]
117. Kim, S.; Hwang, H.J.; Cho, H.; Choi, D.; Hwang, W. Repeatable replication method with liquid infiltration to fabricate robust, flexible, and transparent, anti-reflective superhydrophobic polymer films on a large scale. *Chem. Eng. J.* **2018**, *350*, 225–232. [[CrossRef](#)]
118. Kim, S.; Cho, H.; Hwang, W. Simple fabrication method of flexible and translucent high-aspect ratio superhydrophobic polymer tube using a repeatable replication and nondestructive detachment process. *Chem. Eng. J.* **2019**, *361*, 975–981. [[CrossRef](#)]
119. Li, X.; Gao, L.; Wang, M.; Lv, D.; He, P.; Xie, Y.; Zhan, X.; Li, J.; Lin, Z. Recent development and emerging applications of robust biomimetic superhydrophobic wood. *J. Mater. Chem. A* **2023**, *11*, 6772–6795. [[CrossRef](#)]
120. Hooda, A.; Goyat, M.S.; Pandey, J.K.; Kumar, A.; Gupta, R. A review on fundamentals, constraints and fabrication techniques of superhydrophobic coatings. *Prog. Org. Coat.* **2020**, *142*, 105557. [[CrossRef](#)]
121. Escorcia-Díaz, D.; García-Mora, S.; Rendón-Castrillón, L.; Ramírez-Carmona, M.; Ocampo-López, C. Advancements in Nanoparticle Deposition Techniques for Diverse Substrates: A Review. *Nanomaterials* **2023**, *13*, 2586. [[CrossRef](#)]
122. Gudmundsson, J.T.; Anders, A.; von Keudell, A. Foundations of physical vapor deposition with plasma assistance. *Plasma Sources Sci. Technol.* **2022**, *31*, 083001. [[CrossRef](#)]
123. Li, J.; Li, C.-X.; Chen, Q.-Y.; Gao, J.-T.; Wang, J.; Yang, G.-J.; Li, C.-J. Super-Hydrophobic Surface Prepared by Lanthanide Oxide Ceramic Deposition Through PS-PVD Process. *J. Therm. Spray Technol.* **2017**, *26*, 398–408. [[CrossRef](#)]
124. Gao, W.; Ma, F.; Yin, Y.; Li, J. Robust and durable transparent superhydrophobic F-TNTs/TiN coating fabricated by structure tuning on surface of TiN hard coating. *Appl. Surf. Sci.* **2023**, *613*, 155967. [[CrossRef](#)]
125. Wang, W.; Feng, L.; Song, B.; Wang, L.; Shao, R.; Xia, Y.; Liu, D.; Li, T.; Liu, S.; Wang, L.; et al. Fabrication and application of superhydrophobic nonwovens: A review. *Mater. Today Chem.* **2022**, *26*, 101227. [[CrossRef](#)]
126. Marchalot, J.; Ramos, S.M.M.; Pirat, C.; Journet, C. Enhanced water repellency of surfaces coated with multiscale carbon structures. *Appl. Surf. Sci.* **2018**, *428*, 364–369. [[CrossRef](#)]
127. Busa, C. Novel Bottom-Up Sub-Micron Architectures for Advanced Functional Devices. Ph.D. Thesis, University of Birmingham (United Kingdom), Birmingham, UK, 2018.

128. Liang, Z.; Zhou, Z.; Dong, B.; Wang, S. Fabrication of Superhydrophobic and UV-Resistant Silk Fabrics with Laundering Durability and Chemical Stabilities. *Coatings* **2020**, *10*, 349. [[CrossRef](#)]
129. Kalmoni, J.J.; Heale, F.L.; Blackman, C.S.; Parkin, I.P.; Carmalt, C.J. A Single-Step Route to Robust and Fluorine-Free Superhydrophobic Coatings via Aerosol-Assisted Chemical Vapor Deposition. *Langmuir* **2023**, *39*, 7731–7740. [[CrossRef](#)] [[PubMed](#)]
130. Yu, Y.; Cui, W.; Song, L.; Liao, Q.; Ma, K.; Zhong, S.; Yue, H.; Liang, B. Design of Organic-Free Superhydrophobic TiO<sub>2</sub> with Ultraviolet Stability or Ultraviolet-Induced Switchable Wettability. *ACS Appl. Mater. Interfaces* **2022**, *14*, 9864–9872. [[CrossRef](#)] [[PubMed](#)]
131. Kang, H.; Zhao, B.; Li, L.; Zhang, J. Durable superhydrophobic glass wool@polydopamine@PDMS for highly efficient oil/water separation. *J. Colloid Interface Sci.* **2019**, *544*, 257–265. [[CrossRef](#)] [[PubMed](#)]
132. Mosayebi, E.; Azizian, S.; Noei, N. Preparation of Robust Superhydrophobic Sand by Chemical Vapor Deposition of Polydimethylsiloxane for Oil/Water Separation. *Macromol. Mater. Eng.* **2020**, *305*, 2000425. [[CrossRef](#)]
133. Tombesi, A.; Li, S.; Sathasivam, S.; Page, K.; Heale, F.L.; Pettinari, C.; Carmalt, C.J.; Parkin, I.P. Aerosol-assisted chemical vapour deposition of transparent superhydrophobic film by using mixed functional alkoxysilanes. *Sci. Rep.* **2019**, *9*, 7549. [[CrossRef](#)] [[PubMed](#)]
134. Darmanin, T.; de Givenchy, E.T.; Amigoni, S.; Guittard, F. Superhydrophobic Surfaces by Electrochemical Processes. *Adv. Mater.* **2013**, *25*, 1378–1394. [[CrossRef](#)] [[PubMed](#)]
135. Xie, Z.; Wang, H.; Geng, Y.; Li, M.; Deng, Q.; Tian, Y.; Chen, R.; Zhu, X.; Liao, Q. Carbon-Based Photothermal Superhydrophobic Materials with Hierarchical Structure Enhances the Anti-Icing and Photothermal Deicing Properties. *ACS Appl. Mater. Interfaces* **2021**, *13*, 48308–48321. [[CrossRef](#)] [[PubMed](#)]
136. Yan, Q.; Zhou, S.; Ma, L.; Wan, S.; Zhu, X. Approach to excellent superhydrophobicity and corrosion resistance of carbon-based films by graphene and cobalt synergism. *Surf. Interface Anal.* **2019**, *51*, 152–163. [[CrossRef](#)]
137. Zhu, X.; Zhou, S.; Yan, Q. Ternary graphene/amorphous carbon/nickel nanocomposite film for outstanding superhydrophobicity. *Chem. Phys.* **2018**, *505*, 19–25. [[CrossRef](#)]
138. Chen, F.; Hao, S.; Huang, S.; Lu, Y. Nanoscale SiO<sub>2</sub>-coated superhydrophobic meshes via electro-spray deposition for oil-water separation. *Powder Technol.* **2020**, *373*, 82–92. [[CrossRef](#)]
139. Saji, V.S. Superhydrophobic surfaces and coatings by electrochemical methods—A review. *J. Adhes. Sci. Technol.* **2022**, *37*, 137–161. [[CrossRef](#)]
140. Gan, Z.; Kong, D.; Yu, Q.; Jia, Y.; Dong, X.-H.; Wang, L. Fabrication superhydrophobic composite membranes with hierarchical geometries and low-surface-energy modifications. *Polymer* **2020**, *211*, 123097. [[CrossRef](#)]
141. Cheng, X.Q.; Jiao, Y.; Sun, Z.; Yang, X.; Cheng, Z.; Bai, Q.; Zhang, Y.; Wang, K.; Shao, L. Constructing Scalable Superhydrophobic Membranes for Ultrafast Water–Oil Separation. *ACS Nano* **2021**, *15*, 3500–3508. [[CrossRef](#)]
142. Raman, A.; Jayan, J.S.; Deeraj, B.D.S.; Saritha, A.; Joseph, K. Electrospun Nanofibers as Effective Superhydrophobic Surfaces: A Brief review. *Surf. Interfaces* **2021**, *24*, 101140. [[CrossRef](#)]
143. Kim, T.; Song, M.G.; Kim, K.; Jeon, H.; Kim, G.H. Recyclable Superhydrophobic Surface Prepared via Electrospinning and Electrospinning Using Waste Polyethylene Terephthalate for Self-Cleaning Applications. *Polymers* **2023**, *15*, 3810. [[CrossRef](#)] [[PubMed](#)]
144. Jin, C.; Gong, X.; Jiao, W.; Yin, X.; Yu, J.; Zhang, S.; Ding, B. Superhydrophobic polyvinylidene fluoride nanofibrous membranes with stable hierarchical structures for protective textiles. *Compos. Commun.* **2023**, *38*, 101500. [[CrossRef](#)]
145. Wei, Z.; Teng, S.; Fu, Y.; Zhou, Q.; Yang, W. Micro/nano-structured electrospun membranes with superhydrophobic and photodynamic antibacterial performances. *Prog. Org. Coat.* **2022**, *164*, 106703. [[CrossRef](#)]
146. Ding, L.; Chen, M.; Lu, H.; He, H.; Liu, X.; Wang, Y. 3D multiscale sponges with plant-inspired controllable superhydrophobic coating for oil spill cleanup. *Prog. Org. Coat.* **2021**, *151*, 106075. [[CrossRef](#)]
147. Celik, N.; Torun, I.; Ruzi, M.; Esidir, A.; Onses, M.S. Fabrication of robust superhydrophobic surfaces by one-step spray coating: Evaporation driven self-assembly of wax and nanoparticles into hierarchical structures. *Chem. Eng. J.* **2020**, *396*, 125230. [[CrossRef](#)]
148. Lyu, J.; Wu, B.; Wu, N.; Peng, C.; Yang, J.; Meng, Y.; Xing, S. Green preparation of transparent superhydrophobic coatings with persistent dynamic impact resistance for outdoor applications. *Chem. Eng. J.* **2021**, *404*, 126456. [[CrossRef](#)]
149. Hou, D.; Christie, K.S.S.; Wang, K.; Tang, M.; Wang, D.; Wang, J. Biomimetic superhydrophobic membrane for membrane distillation with robust wetting and fouling resistance. *J. Membr. Sci.* **2020**, *599*, 117708. [[CrossRef](#)]
150. Tang, S.; Wu, Z.; Feng, G.; Wei, L.; Weng, J.; Ruiz-Hitzky, E.; Wang, X. Multifunctional sandwich-like composite film based on superhydrophobic MXene for self-cleaning, photodynamic and antimicrobial applications. *Chem. Eng. J.* **2023**, *454*, 140457. [[CrossRef](#)]
151. Wang, P.; Yang, Y.; Wang, H.; Wang, H. Fabrication of super-robust and nonfluorinated superhydrophobic coating based on diatomaceous earth. *Surf. Coat. Technol.* **2019**, *362*, 90–96. [[CrossRef](#)]
152. Chen, Q.; de Leon, A.; Advincula, R.C. Inorganic–Organic Thiol–ene Coated Mesh for Oil/Water Separation. *ACS Appl. Mater. Interfaces* **2015**, *7*, 18566–18573. [[CrossRef](#)]
153. Qi, C.; Chen, H.; Sun, Y.; Shen, L.; Li, X.; Fu, Q.; Liu, Y. Facile preparation of robust superhydrophobic surface based on multi-scales nanoparticle. *Polym. Eng. Sci.* **2020**, *60*, 1785–1794. [[CrossRef](#)]

154. Zhu, Y.; Pei, L.; Ambreen, J.; He, C.; Ngai, T. Facile Preparation of a Fluorine-Free, Robust, Superhydrophobic Coating through Dip Coating Combined with Non-Solvent Induced Phase Separation (Dip-Coating-NIPS) Method. *Macromol. Chem. Phys.* **2020**, *221*, 2000023. [[CrossRef](#)]
155. Wang, P.; Yao, T.; Li, Z.; Wei, W.; Xie, Q.; Duan, W.; Han, H. A superhydrophobic/electrothermal synergistically anti-icing strategy based on graphene composite. *Compos. Sci. Technol.* **2020**, *198*, 108307. [[CrossRef](#)]
156. Chen, W.; Huang, X.; Zhou, M.; Liu, H.; Xu, M.; Zhu, J. Rose-petal-inspired fabrication of conductive superhydrophobic/superoleophilic carbon with high adhesion to water from orange peels for efficient oil adsorption from oil-water emulsion. *Colloids Surf. A Physicochem. Eng. Asp.* **2023**, *661*, 130920. [[CrossRef](#)]
157. Gu, W.; Li, W.; Zhang, Y.; Xia, Y.; Wang, Q.; Wang, W.; Liu, P.; Yu, X.; He, H.; Liang, C.; et al. Ultra-durable superhydrophobic cellular coatings. *Nat. Commun.* **2023**, *14*, 5953. [[CrossRef](#)] [[PubMed](#)]
158. Zhang, G.-D.; Wu, Z.-H.; Xia, Q.-Q.; Qu, Y.-X.; Pan, H.-T.; Hu, W.-J.; Zhao, L.; Cao, K.; Chen, E.-Y.; Yuan, Z.; et al. Ultrafast Flame-Induced Pyrolysis of Poly(dimethylsiloxane) Foam Materials toward Exceptional Superhydrophobic Surfaces and Reliable Mechanical Robustness. *ACS Appl. Mater. Interfaces* **2021**, *13*, 23161–23172. [[CrossRef](#)] [[PubMed](#)]
159. Ruzi, M.; Celik, N.; Onses, M.S. Superhydrophobic coatings for food packaging applications: A review. *Food Packag. Shelf Life* **2022**, *32*, 100823. [[CrossRef](#)]
160. Dalawai, S.P.; Saad Aly, M.A.; Latthe, S.S.; Xing, R.; Sutar, R.S.; Nagappan, S.; Ha, C.-S.; Kumar Sadasivuni, K.; Liu, S. Recent Advances in durability of superhydrophobic self-cleaning technology: A critical review. *Prog. Org. Coat.* **2020**, *138*, 105381. [[CrossRef](#)]
161. Zhao, H.; Gao, W.-C.; Li, Q.; Khan, M.R.; Hu, G.-H.; Liu, Y.; Wu, W.; Huang, C.-X.; Li, R.K.Y. Recent advances in superhydrophobic polyurethane: Preparations and applications. *Adv. Colloid Interface Sci.* **2022**, *303*, 102644. [[CrossRef](#)]
162. Li, B.; Bai, J.; He, J.; Ding, C.; Dai, X.; Ci, W.; Zhu, T.; Liao, R.; Yuan, Y. A Review on Superhydrophobic Surface with Anti-Icing Properties in Overhead Transmission Lines. *Coatings* **2023**, *13*, 301. [[CrossRef](#)]
163. Li, W.; Zhan, Y.; Yu, S. Applications of superhydrophobic coatings in anti-icing: Theory, mechanisms, impact factors, challenges and perspectives. *Prog. Org. Coat.* **2021**, *152*, 106117. [[CrossRef](#)]
164. Golovin, K.; Dhyani, A.; Thouless, M.D.; Tuteja, A. Low-interfacial toughness materials for effective large-scale deicing. *Science* **2019**, *364*, 371–375. [[CrossRef](#)] [[PubMed](#)]
165. Hou, Y.; Yu, M.; Shang, Y.; Zhou, P.; Song, R.; Xu, X.; Chen, X.; Wang, Z.; Yao, S. Suppressing Ice Nucleation of Supercooled Condensate with Biphilic Topography. *Phys. Rev. Lett.* **2018**, *120*, 075902. [[CrossRef](#)] [[PubMed](#)]
166. Tao, B.; Cheng, L.; Wang, J.; Zhang, X.; Liao, R. A review on mechanism and application of functional coatings for overhead transmission lines. *Front. Mater.* **2022**, *9*, 995290. [[CrossRef](#)]
167. Cao, Y.; Tan, W.; Wu, Z. Aircraft icing: An ongoing threat to aviation safety. *Aerosp. Sci. Technol.* **2018**, *75*, 353–385. [[CrossRef](#)]
168. Meuler, A.J.; McKinley, G.H.; Cohen, R.E. Exploiting Topographical Texture To Impart Icephobicity. *ACS Nano* **2010**, *4*, 7048–7052. [[CrossRef](#)] [[PubMed](#)]
169. Gao, H.; Jian, Y.; Yan, Y. The effects of bio-inspired micro/nano scale structures on anti-icing properties. *Soft Matter* **2021**, *17*, 447–466. [[CrossRef](#)] [[PubMed](#)]
170. Lin, Y.; Chen, H.; Wang, G.; Liu, A. Recent Progress in Preparation and Anti-Icing Applications of Superhydrophobic Coatings. *Coatings* **2018**, *8*, 208. [[CrossRef](#)]
171. Wang, L.; Zhao, H.; Zhu, D.; Yuan, L.; Zhang, H.; Fan, P.; Zhong, M. A Review on Ultrafast Laser Enabled Excellent Superhydrophobic Anti-Icing Performances. *Appl. Sci.* **2023**, *13*, 5478. [[CrossRef](#)]
172. Kreder, M.J.; Alvarenga, J.; Kim, P.; Aizenberg, J. Design of anti-icing surfaces: Smooth, textured or slippery? *Nat. Rev. Mater.* **2016**, *1*, 15003. [[CrossRef](#)]
173. Pan, L.; Xue, P.; Wang, M.; Wang, F.; Guo, H.; Yuan, X.; Zhong, L.; Yu, J. Novel superhydrophobic carbon fiber/epoxy composites with anti-icing properties. *J. Mater. Res.* **2021**, *36*, 1695–1704. [[CrossRef](#)]
174. Tong, W.; Xiong, D.; Wang, N.; Wu, Z.; Zhou, H. Mechanically robust superhydrophobic coating for aeronautical composite against ice accretion and ice adhesion. *Compos. Part B Eng.* **2019**, *176*, 107267. [[CrossRef](#)]
175. Zhang, H.; Zhang, X.; He, F.; Lv, C.; Hao, P. How micropatterns affect the anti-icing performance of superhydrophobic surfaces. *Int. J. Heat Mass Transf.* **2022**, *195*, 123196. [[CrossRef](#)]
176. Zhang, Z.; Zhou, J.; Ren, Y.; Li, W.; Li, S.; Chai, N.; Zeng, Z.; Chen, X.; Yue, Y.; Zhou, L.; et al. Passive Deicing CFRP Surfaces Enabled by Super-Hydrophobic Multi-Scale Micro-Nano Structures Fabricated via Femtosecond Laser Direct Writing. *Nanomaterials* **2022**, *12*, 2782. [[CrossRef](#)] [[PubMed](#)]
177. Li, J.; Wang, W.; Zhu, R.; Huang, Y. Fabrication and characterization of multiscale spherical artificial compound eye with self-cleaning and anti-icing properties. *Results Phys.* **2021**, *24*, 104153. [[CrossRef](#)]
178. Li, J.; Wang, W.; Mei, X.; Pan, A.; Sun, X.; Liu, B.; Cui, J. Artificial Compound Eyes Prepared by a Combination of Air-Assisted Deformation, Modified Laser Swelling, and Controlled Crystal Growth. *ACS Nano* **2019**, *13*, 114–124. [[CrossRef](#)] [[PubMed](#)]
179. Wang, Y.; Zhang, J.; Dodiuk, H.; Kenig, S.; Ratto, J.A.; Barry, C.; Mead, J. The reduction in ice adhesion using controlled topography superhydrophobic coatings. *J. Coat. Technol. Res.* **2023**, *20*, 469–483. [[CrossRef](#)]
180. Deng, L.; Wang, Z.; Niu, Y.; Luo, F.; Chen, Q. CNTs-induced superhydrophobic and photothermal coating with long-term durability and self-replenishing property for anti-icing/de-icing. *Compos. Sci. Technol.* **2024**, *245*, 110347. [[CrossRef](#)]

181. Tian, Y.; Xu, Y.; Zhu, Z.; Liu, Y.; Xie, J.; Zhang, B.; Zhang, H.; Zhang, Q. Hierarchical micro/nano/porous structure PVDF/hydrophobic GO photothermal membrane with highly efficient anti-icing/de-icing performance. *Colloids Surf. A Physicochem. Eng. Asp.* **2022**, *651*, 129586. [[CrossRef](#)]
182. Jiang, G.; Liu, Z.; Hu, J. Superhydrophobic and Photothermal PVDF/CNTs Durable Composite Coatings for Passive Anti-Icing/Active De-Icing. *Adv. Mater. Interfaces* **2022**, *9*, 2101704. [[CrossRef](#)]
183. Lee, J.-S.; Hoang, V.-T.; Kweon, J.-H.; Nam, Y.-W. Multifunctional Ni-plated carbon fiber reinforced thermoplastic composite with excellent electrothermal and superhydrophobic properties using MWCNTs and SiO<sub>2</sub>/Ag microspheres. *Compos. Part A Appl. Sci. Manuf.* **2023**, *171*, 107585. [[CrossRef](#)]
184. Beyer, J.; Goksøyr, A.; Hjermmann, D.Ø.; Klungsoyr, J. Environmental effects of offshore produced water discharges: A review focused on the Norwegian continental shelf. *Mar. Environ. Res.* **2020**, *162*, 105155. [[CrossRef](#)] [[PubMed](#)]
185. Broch, O.J.; Nepstad, R.; Ellingsen, I.; Bast, R.; Skeie, G.M.; Carroll, J. Simulating crude oil exposure, uptake and effects in North Atlantic Calanus finmarchicus populations. *Mar. Environ. Res.* **2020**, *162*, 105184. [[CrossRef](#)] [[PubMed](#)]
186. Teal, J.M.; Howarth, R.W. Oil spill studies: A review of ecological effects. *Environ. Manag.* **1984**, *8*, 27–43. [[CrossRef](#)]
187. Xiong, Q.; Tian, Q.; Yue, X.; Xu, J.; He, X.; Qiu, F.; Zhang, T. Superhydrophobic PET@ZnO Nanofibrous Membrane Extract from Waste Plastic for Efficient Water-In-Oil Emulsion Separation. *Ind. Eng. Chem. Res.* **2022**, *61*, 11804–11814. [[CrossRef](#)]
188. Zhang, Y.; Wang, X.; Wang, C.; Zhai, H.; Liu, B.; Zhao, X.; Fang, D.; Wei, Y. Facile preparation of flexible and stable superhydrophobic non-woven fabric for efficient oily wastewater treatment. *Surf. Coat. Technol.* **2019**, *357*, 526–534. [[CrossRef](#)]
189. Huang, G.; Lai, B.; Xu, H.; Jin, Y.; Huo, L.; Li, Z.; Deng, Y. Fabrication of a superhydrophobic fabric with a uniform hierarchical structure via a bottom-blown stirring method for highly efficient oil–water separation. *Sep. Purif. Technol.* **2021**, *258*, 118063. [[CrossRef](#)]
190. Zhang, W.; Lu, X.; Xin, Z.; Zhou, C. A self-cleaning polybenzoxazine/TiO<sub>2</sub> surface with superhydrophobicity and superoleophilicity for oil/water separation. *Nanoscale* **2015**, *7*, 19476–19483. [[CrossRef](#)] [[PubMed](#)]
191. Shen, L.; Wang, X.; Zhang, Z.; Jin, X.; Jiang, M.; Zhang, J. Design and Fabrication of the Evolved Zeolitic Imidazolate Framework-Modified Polylactic Acid Nonwoven Fabric for Efficient Oil/Water Separation. *ACS Appl. Mater. Interfaces* **2021**, *13*, 14653–14661. [[CrossRef](#)]
192. Cui, C.; Wang, W.; Lv, X.; Jiao, S.; Pang, G. Fabrication of superwetting non-woven fabric by grafting one-dimensional inorganic nanostructure for efficient separation of surfactant-stabilized organic solvent/water emulsions. *Colloids Surf. A Physicochem. Eng. Asp.* **2023**, *663*, 131068. [[CrossRef](#)]
193. Yuan, H.; Zhang, M.; Pan, Y.; Liu, C.; Shen, C.; Chen, Q.; Liu, X. Microspheres Modified with Superhydrophobic Non-Woven Fabric with High-Efficiency Oil–Water Separation: Controlled Water Content in PLA Solution. *Macromol. Mater. Eng.* **2022**, *307*, 2100919. [[CrossRef](#)]
194. Abu-Thabit, N.Y.; Azad, A.K.; Mezghani, K.; Hakeem, A.S.; Drmosh, Q.A.; Akhtar, S.; Adesina, A.Y. Facile and Green Fabrication of Superhydrophobic Polyacrylonitrile Nonwoven Fabric with Iron Hydroxide Nanoparticles for Efficient Oil/Water Separation. *ACS Appl. Polym. Mater.* **2022**, *4*, 8450–8460. [[CrossRef](#)]
195. Kim, D.-S.; Kang, J.; Jung, J.-Y.; Hwang, M.; Seo, S.; Kim, J.-H. Facile Fabrication of Superhydrophobic Polymer Membranes with Hierarchical Structure for Efficient Oil/Water Separation. *Fibers Polym.* **2022**, *23*, 2365–2372. [[CrossRef](#)]
196. Wei, J.; Nian, P.; Wang, Y.; Wang, X.; Wang, Y.; Xu, N.; Wei, Y. Preparation of superhydrophobic-superoleophilic ZnO nanoflower@SiC composite ceramic membranes for water-in-oil emulsion separation. *Sep. Purif. Technol.* **2022**, *292*, 121002. [[CrossRef](#)]
197. Wei, Y.; Xie, Z.; Qi, H. Superhydrophobic-superoleophilic SiC membranes with micro-nano hierarchical structures for high-efficient water-in-oil emulsion separation. *J. Membr. Sci.* **2020**, *601*, 117842. [[CrossRef](#)]
198. Ifelebuegu, A.; Lale, E.; Mbanaso, F.; Theophilus, S. Facile Fabrication of Recyclable, Superhydrophobic, and Oleophilic Sorbent from Waste Cigarette Filters for the Sequestration of Oil Pollutants from an Aqueous Environment. *Processes* **2018**, *6*, 140. [[CrossRef](#)]
199. Gao, X.; Yan, X.; Yao, X.; Xu, L.; Zhang, K.; Zhang, J.; Yang, B.; Jiang, L. The Dry-Style Antifogging Properties of Mosquito Compound Eyes and Artificial Analogues Prepared by Soft Lithography. *Adv. Mater.* **2007**, *19*, 2213–2217. [[CrossRef](#)]
200. Niu, H.; Luo, S.; Yao, X.; Li, T.; Ai, M.; Zhou, R.; Wang, H.; Wan, L.; Du, Y.; Hu, L.; et al. A review of transparent superhydrophobic materials and their research in the field of photovoltaic dust removal. *Mater. Sci. Semicond. Process.* **2023**, *166*, 107741. [[CrossRef](#)]
201. Li, J.; Zheng, J.Y.; Zhang, J.; Feng, J. Fabrication of TiO<sub>2</sub>/PU Superhydrophobic Film by Nanoparticle Assisted Cast Micromolding Process. *J. Nanosci. Nanotechnol.* **2016**, *16*, 5875–5879. [[CrossRef](#)]
202. Liu, S.; Han, Y.; Qie, J.; Chen, S.; Liu, D.; Duo, L.; Chen, H.; Lin, Q. Environment friendly superhydrophobic and transparent surface coating via layer-by-layer self-assembly for antifogging of optical lenses. *J. Biomater. Sci. Polym. Ed.* **2021**, *33*, 847–857. [[CrossRef](#)]
203. Xi, R.; Wang, Y.; Wang, X.; Lv, J.; Li, X.; Li, T.; Zhang, X.; Du, X. Ultrafine nano-TiO<sub>2</sub> loaded on dendritic porous silica nanoparticles for robust transparent antifogging self-cleaning nanocoatings. *Ceram. Int.* **2020**, *46*, 23651–23661. [[CrossRef](#)]
204. Wooh, S.; Koh, J.H.; Lee, S.; Yoon, H.; Char, K. Trilevel-Structured Superhydrophobic Pillar Arrays with Tunable Optical Functions. *Adv. Funct. Mater.* **2014**, *24*, 5550–5556. [[CrossRef](#)]
205. Passoni, L.; Bonvini, G.; Luzio, A.; Facibeni, A.; Bottani, C.E.; Di Fonzo, F. Multiscale Effect of Hierarchical Self-Assembled Nanostructures on Superhydrophobic Surface. *Langmuir* **2014**, *30*, 13581–13587. [[CrossRef](#)]

206. SHU, Z.; BAO, J.; CHEN, B.; HE, J.; JIE, J.; PU, M. Research on Anti-ice Performance of a Novel ZnO/SiO<sub>2</sub> Composite Superhydrophobic Coating Modified by Magnetron Sputtering and Fluoridation. *Surf. Technol.* **2022**, *51*, 452–459. [[CrossRef](#)]
207. Lai, C.-J.; Chen, Y.-J.; Wu, M.-X.; Wu, C.-C.; Tang, N.-T.; Hsu, T.-F.; Lin, S.-H.; Li, H.-F.; Yang, H. Self-cleaning and anti-fogging hierarchical structure arrays inspired by termite wing. *Appl. Surf. Sci.* **2023**, *616*, 156484. [[CrossRef](#)]
208. Wang, T.; Zhang, C.; Wang, H.; Liu, Y.; Wang, J.; Shi, Z. Ultra-high performance flexible and controllable superhydrophobic films based on microsphere/micro-pyramid hierarchical arrays. *Colloids Surf. A Physicochem. Eng. Asp.* **2023**, *677*, 132449. [[CrossRef](#)]
209. Li, W.; Chen, Y.; Jiao, Z. Efficient Anti-Fog and Anti-Reflection Functions of the Bio-Inspired, Hierarchically-Architected Surfaces of Multiscale Columnar Structures. *Nanomaterials* **2023**, *13*, 1570. [[CrossRef](#)] [[PubMed](#)]
210. Jang, N.-S.; Ha, S.-H.; Kim, K.-H.; Kim, J.-M. Facile one-step photopatterning of hierarchical polymer structures for highly transparent, flexible superhydrophobic films. *Prog. Org. Coat.* **2019**, *130*, 24–30. [[CrossRef](#)]
211. Liu, P.; Niu, L.; Tao, X.; Li, X.; Zhang, Z. Hydrophobic Silica with Potential for Water-Injection Augmentation of a Low-Permeability Reservoir: Drag Reduction and Self-Cleaning Ability in Relation to Interfacial Interactions. *ACS Omega* **2019**, *4*, 13681–13686. [[CrossRef](#)]
212. Tian, N.; Chen, K.; Yu, H.; Wei, J.; Zhang, J. Super pressure-resistant superhydrophobic fabrics with real self-cleaning performance. *iScience* **2022**, *25*, 104494. [[CrossRef](#)]
213. Maharjan, S.; Liao, K.-S.; Wang, A.J.; Barton, K.; Haldar, A.; Alley, N.J.; Byrne, H.J.; Curran, S.A. Self-cleaning hydrophobic nanocoating on glass: A scalable manufacturing process. *Mater. Chem. Phys.* **2020**, *239*, 122000. [[CrossRef](#)]
214. Shi, S.; Wang, X.; Li, Z.; Meng, J.; Chu, X.; Zhang, P.; Sun, B.; Zhang, J.; Gao, Y.; Xu, W.; et al. Multifunctional Integrated Superhydrophobic Coatings with Unique Fluorescence and Micro/Micro/Nano-Hierarchical Structures Enabled by In Situ Self-Assembly. *ACS Appl. Mater. Interfaces* **2023**, *15*, 7442–7453. [[CrossRef](#)] [[PubMed](#)]
215. Liu, G.; Zhao, T.; Fei, H.; Li, F.; Guo, W.; Yao, Z.; Feng, Z. A review of various self-cleaning surfaces, durability and functional applications on building exteriors. *Constr. Build. Mater.* **2023**, *409*, 134084. [[CrossRef](#)]
216. Oh, S.; Cho, J.W.; Lee, J.; Han, J.; Kim, S.K.; Nam, Y. A Scalable Haze-Free Antireflective Hierarchical Surface with Self-Cleaning Capability. *Adv. Sci.* **2022**, *9*, 2202781. [[CrossRef](#)] [[PubMed](#)]
217. Sutar, R.S.; Shi, B.; Kanchankoti, S.S.; Ingole, S.S.; Jamadar, W.S.; Sayyad, A.J.; Khot, P.B.; Sadasivuni, K.K.; Latthe, S.S.; Liu, S.; et al. Development of self-cleaning superhydrophobic cotton fabric through silica/PDMS composite coating. *Surf. Topogr. Metrol. Prop.* **2023**, *11*, 045004. [[CrossRef](#)]
218. Oh, J.H.; Park, C.H. The Effect of Fiber Type and Yarn Diameter on Superhydrophobicity, Self-Cleaning Property, and Water Spray Resistance. *Polymers* **2021**, *13*, 817. [[CrossRef](#)] [[PubMed](#)]
219. Pakdel, E.; Zhao, H.; Wang, J.; Tang, B.; Varley, R.J.; Wang, X. Superhydrophobic and photocatalytic self-cleaning cotton fabric using flower-like N-doped TiO<sub>2</sub>/PDMS coating. *Cellulose* **2021**, *28*, 8807–8820. [[CrossRef](#)]
220. Altangerel, Z.; Purev-Ochir, B.; Ganzorig, A.; Tsagaantsooj, T.; Lkhamsuren, G.; Choisuren, A.; Chimed, G. Superhydrophobic modification and characterization of cashmere fiber surfaces by wet coating techniques of silica nanoparticles. *Surf. Interfaces* **2020**, *19*, 100533. [[CrossRef](#)]
221. Luo, W.; Sun, D.; Chen, S.; Shanmugam, L.; Xiang, Y.; Yang, J. Robust Microcapsules with Durable Superhydrophobicity and Superoleophilicity for Efficient Oil–Water Separation. *ACS Appl. Mater. Interfaces* **2020**, *12*, 57547–57559. [[CrossRef](#)]
222. Teh, S.-Y.; Lin, R.; Hung, L.-H.; Lee, A.P. Droplet microfluidics. *Lab A Chip* **2008**, *8*, 198–220. [[CrossRef](#)]
223. Jiao, L.; Wu, Y.; Hu, Y.; Wu, H.; Xu, Z.; Han, L.; Guo, Q.; Li, D.; Chen, R. Oil/Water Microreactor with a Core–Shell Wetting State on a SOB/OL-SHB/HL Multilevel Patterned Surface. *J. Phys. Chem. C* **2021**, *125*, 27771–27783. [[CrossRef](#)]
224. Wang, W.; Lai, H.; Cheng, Z.; Fan, Z.; Zhang, D.; Wang, J.; Yu, S.; Xie, Z.; Liu, Y. Superhydrophobic Shape Memory Polymer Microarrays with Switchable Directional/Antidirectional Droplet Sliding and Optical Performance. *ACS Appl. Mater. Interfaces* **2020**, *12*, 49219–49226. [[CrossRef](#)] [[PubMed](#)]
225. Nokes, J.; Sharma, H.; Tu, R.; Kim, M.; Chu, M.; Siddiqui, A.; Khine, M. Nanotextured Shrink Wrap Superhydrophobic Surfaces by Argon Plasma Etching. *Materials* **2016**, *9*, 196. [[CrossRef](#)] [[PubMed](#)]
226. Li, Y.; Bi, J.; Wang, S.; Zhang, T.; Xu, X.; Wang, H.; Cheng, S.; Zhu, B.-W.; Tan, M. Bio-inspired Edible Superhydrophobic Interface for Reducing Residual Liquid Food. *J. Agric. Food Chem.* **2018**, *66*, 2143–2150. [[CrossRef](#)] [[PubMed](#)]

**Disclaimer/Publisher’s Note:** The statements, opinions and data contained in all publications are solely those of the individual author(s) and contributor(s) and not of MDPI and/or the editor(s). MDPI and/or the editor(s) disclaim responsibility for any injury to people or property resulting from any ideas, methods, instructions or products referred to in the content.